2015-08-01

Ribosome Component Turnover Kinetics Describes a Two-Pool Kinetic Model in Dietary Restriction that Suggests RPL10 is Exchanged During Ribosome Lifespan

Andrew David Mathis
Brigham Young University

Ribosome Component Turnover Kinetics Describes a Two-Pool Kinetic Model in Dietary Restriction That Suggests RPL10 is Exchanged During Ribosome Lifespan

Andrew David Mathis

A thesis submitted to the faculty of
Brigham Young University
in partial fulfillment of the requirements for the degree of

Master of Science

John C. Price, Chair
Barry M. Willardson
Natalie J. Blades

Department of Chemistry and Biochemistry

Brigham Young University

August 2015

ABSTRACT

Ribosome Component Turnover Kinetics Describes a Two-Pool Kinetic Model in Dietary Restriction That Suggests RPL10 is Exchanged During Ribosome Lifespan

Andrew David Mathis
Department of Chemistry and Biochemistry, BYU
Master of Science

The eukaryotic ribosome is a large molecular machine consisting of ~80 ribosomal proteins and 4 rRNAs. The 40S and 60S ribosomal subunits are assembled in the nucleolus by ~200 helper proteins then shipped into the cytoplasm or to the endoplasmic reticulum where protein translation takes place. Eventually ribosomes are removed from the cytoplasm and recycled through ribophagy, however, very is little is known about ribosomal protein exchange after assembly but before ribophagy. Using kinetic turnover measurements of ribosomal proteins and rRNA *in vivo* we determined ribosomal protein replacement rates are diverse suggesting ribosomal components may be replaced without destruction of the entire ribosome. Measurements from *ad libitum* fed and dietary restricted mice provide strong evidence that RPL10 exchanges rates are dramatically different between AL and DR while synthesis and degradation do ont change. RPL10 turnover can be described using a two-pool kinetic model, which may be applied to many ribosomal proteins.

Keywords: ribosome, ribophagy, turnover, kinetics, proteomics, mass spectrometry, dietary restriction

ACKNOWLEDGEMENTS

I acknowledge all those who have taught and trained me as a scientific researcher during my time at Brigham Young University. Specific thanks goes to my fellow graduate student Bradley Naylor who performed the total pool turnover analysis, my committee members Dr. Natalie Blades and Dr. Barry Willardson for their advice and council during my thesis work, and my undergraduate mentor Dr. John Prince who gave me tremendous opportunities to gain experience and succeed. My advisor Dr. John Price has provided incredible insight and support through countless hours of patient mentoring. His influence over the last two years has greatly enhanced my scientific skillset and fostered my abilities to think critically, solve problems, and ask questions. JC has also been a shining example of balancing expectation and kindness. I also thank my parents for their ongoing support and love. Lastly, I express my gratitude to God, who makes all this possible and whose work we study.

TABLE OF CONTENTS

LIST OF FIGURES

Chapter 1: Introduction

1.1 Homeostasis in Biological Systems

Biological homeostasis is required to maintain life. Biological systems are at true homeostasis when biomolecule concentrations are constant. This does not mean the cell is static, rather concentrations are constant because biomolecules are being created and destroyed at the same rate. This rate is often called a turnover or replacement rate. When stimulus pushes biological systems from homeostasis, biomolecule concentrations change. These changes can be caused at three basic levels: 1) Biomolecule synthesis has changed. 2) Biomolecule structure has changed non-covalently. 3) Biomolecule degradation has changed. In the short term this imbalance is positive allowing many necessary biological processes to occur including damaged biomolecule replacement, hormone signaling and energy production.[1] However, if a homeostasis is not reestablished the organism will eventually die. Further, many disease states result in a new homeostasis, which is at least temporarily survivable but can cause a significant loss of fitness.

Currently, most molecular, cellular and biochemical studies measure changes in homeostasis based on biomolecule function, location, and concentration. Though these measurements are very informative and have led to significant biological discovery, we propose current research efforts can be greatly complimented by global turnover analysis, which allows discovery analysis of biomolecule replacement rates. Herein we describe the unique insights gained from combining structural, quantitative, and turnover measurements to explore ribosome homeostasis.

1.2 Making Turnover Measurements

Turnover analysis measures the rate at which old biomolecules are replaced by new biomolecules using a tracer and a detector. At the most basic level a turnover analysis experiment has three requirements: 1. A system with detectable biomolecule turnover. 2. A tracer to label newly synthesized biomolecules 3. A method to detect biomolecules of interest. Requirement 1 is any living biological system and even some synthetic systems, so long as turnover is at a measureable rate. Requirement 2 is often an unnatural concentration of a radioactive or stable isotope, but may also be a chemically derivatized biomolecule. Isotope choice is dependent on the biological system and desired outcomes. Requirement 3 is any method that can identify the biomolecule of interest, as long as it is compatible with isotope detection.

Isotopes are popular tracers in turnover studies because they behave almost identically in biological systems.[1,2] The big exception being radioisotopes that have similar chemical properties, but emit radiation. Further, natural isotope abundances are very predictable, so a shift in natural isotope abundance is fairly easy to discern. Lastly, isotopes can be easily delivered by incorporation into precursor molecules like amino acids or water then administered to cell cultures or animals.

Traditionally, the most common turnover analysis uses ^{35}S methionine[3] enriched culture media to track protein turnover rates over a time course using a radiation detector and immunoprecipitation. In a similar vein ^{3}H or ^{14}C analysis can be used to track nucleobases and metabolites in addition to proteins if an identification method exists for the target molecule.[2,4,5] Turnover analysis using radiolabels is very sensitive and therefore can detect small amounts of change allowing for shorter experiments compared to using stable isotope labeling. Radioisotope methods, especially ^{35}S methionine experiments, are well established and can be performed with

fairly little technical training compared to stable isotope methods. However, radio isotope techniques have three major limitations: 1. Radio isotope approaches are not easily used on an "omic" scale because an independent experiment must be used to identify target molecules. 2. The percent new protein is unknown because the radio-label gives no metric of total protein concentration, and the detection method does not interface quantitatively with the radiolabel. 3. Current radio isotope experiments are generally limited to cell culture because of safety issues in higher level organisms.

Stable isotope labeling methods can be performed on an "omic" scale and in higher organisms including humans.[6] For protein turnover experiments, heavy-labeled synthetic amino acids or D_2O is generally used. Heavy labeled amino acids are incorporated into protein directly. D_2O is incorporated into amino acids through natural biosynthetic pathways *in vivo* and these metabolically labeled amino acids are incorporated into new proteins. Both methods cause unnatural but predictable shifts in peptide isotope patterns that can be quantified using mass spectrometry.[7] The ratio of new protein is established by comparing the unlabeled protein (old) and the labeled protein (new). In this way new protein can be put into the context of total protein and the turnover rate can be directly measured. Further, the mass spectrometer can provide identification information ameliorating the need for a different identification assay and allowing for untargeted discovery. Lastly, stable isotopes are widely accepted for use in higher organisms including humans and have been used in clinical applications allowing turnover measurements to be made in more realistic cellular states.[8] However, moving from basic cell culture to higher compounds the challenge of measuring heavy to light isotope ratios in the precursor pool.[1]

1.3 Solving the Precursor Pool Problem

The precursor pool enrichment must be known to accurately determine turnover rate. For example, let's say one administers D_6-leucine to human patients in order to determine the effects of a new drug on proteasome turnover. D_6-leucine will enter the amino acid precursor pool for protein production, specifically the charged tRNA pool. However, this pool will not be 100% ^{6}D-leucine because endogenous unlabeled leucine does not disappear when ^{6}D-leucine is administered. So, the likelihood of incorporating D_6-leucine into a new protein is based on the ratio of D_6-leucine to endogenous unlabeled leucine. Therefore, if the tRNA leucine precursor pool is 35% ^{6}D-leucine, 100% protein turnover will look like 35% ^{6}D-leucine incorporation, so a 17% increase in D_6-leucine content is 50% new protein. However, if the precursor pool was really 50% D_6-leucine instead of 35% D_6-leucine, a 17% increase in D_6-leucine would correspond to 37% new protein. It is this problem, namely the inability to accurately measure the precursor pool that severely hindered discovery turnover measurements for many years. However, recent advents have provided reliable methods to measure the amino acid precursor pool.[9, 10] One of these methods developed by Price et al. relies upon the reproducible incorporation of water into amino acids.

Using D_2O as an isotope tracer allows the precursor pool to be measured accurately and indirectly in bodily fluids.[9] Briefly, water is involved in the synthesis of most biomolecules, so deuterium from D_2O is naturally incorporated into biomolecules. When deuterium incorporation from water is known, biosynthesis for a given molecule the precursor pool can be accurately described. Further, D_2O is quickly and uniformly distributed throughout the organism, so bodily fluid D_2O enrichment is equivalent in most tissues, whereas, direct administration of heavy labeled amino acids does not provide equal precursor pool enrichment throughout the organism.[11] Equal

D_2O distribution throughout an organism allows precursor pool enrichment to be measured from easily accessible bodily fluids like blood or urine. For these reasons D_2O-based turnover experiments are becoming more popular when studying metabolic changes in higher organisms. Additionally, studies in higher level organisms with slower division rates significantly reduce problems discerning between protein dilution by cell division and protein turnover outside of replication.

Protein production caused by cell replication can mask protein turnover measurements. Every time a cell divides all biomolecules must be duplicated to provide materials for the new cell. Therefore, when working in rapidly dividing cells one must account for doubling rates to measure true protein turnover because noise from the replication signal quickly overcomes protein turnover unassociated with replication. Additionally, long experiments in dividing cell culture are more challenging because changes in growth conditions (high confluence, nutrient depletion, entering or exiting log growth phase) change cellular homeostasis and protein concentration cannot be assumed constant on average. In this case, concentration must be determined in order to truly understand synthesis rate. Concentration data also add significant biological insight to turnover analysis when comparing cellular changes.

1.4 Quantitative and Kinetic Measurements Synergize

Kinetic proteomics can be combined with quantitative proteomics to define within proteome absolute synthesis rates (WPAS), which provide units/time values for biomolecule flux. Kinetic proteomics measure the rate at which a biomolecule is replaced with $time^{-1}$ units. Concentration measurements are generally based upon units of intensity (relative concentration) or grams (absolute concentration). Therefore, the product of turnover rate and concentration is units/time, or WPAS in the case of proteins. WPAS measurements allow a metric of synthesis and

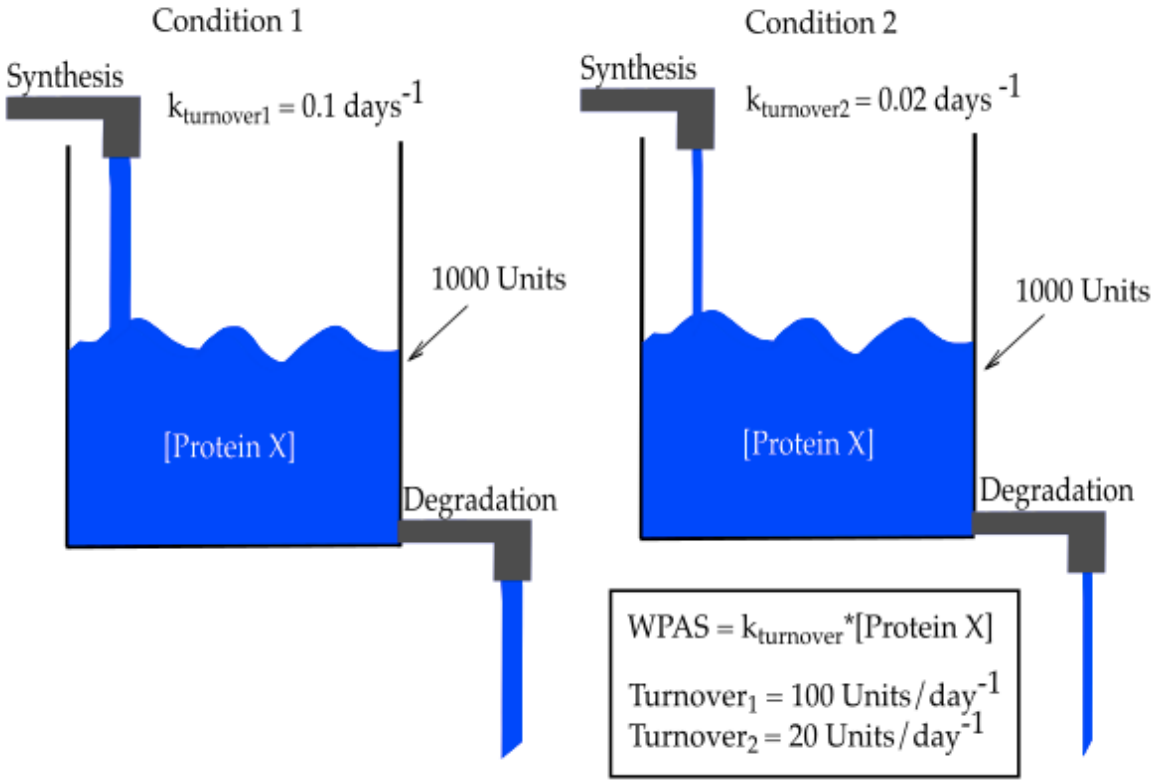

Figure 1: Turnover and Concentration Measurements Synergize

Biomolecule turnover is measured in fraction/day. Concentration is measured units. When combined within-proteome absolute synthesis (WPAS) can be determined. Together these measurements look beyond simple concentration and turnover by putting concentration in the context of turnover and allows quantitative analysis of total synthesis and total degradation rates. Condition 1 and condition 2 both have the same protein concentration, but the turnover measurement shows a decrease in turnover rate in condition 2. The product of concentration and turnover measurements provides a within proteome absolute synthesis rate.

degradation to be valued within concentration measurement. For instance, let us consider the two cellular states in Figure 1. In each state we are measuring protein concentration and protein turnover. We can see that protein x concentration does not change, but turnover does. Change in turnover shows state 1 replaces more protein x per unit time than state 2, or protein x flux is greater in state 1. Because the system is at homeostasis, this combined information describes an environment where both protein synthesis and protein degradation have increased despite stable concentration. This new information drives hypothesis generation. For instance, the protein folding pathway may be damaged or hindered requiring more protein production to maintain the

proper protein working concentration. Recent studies have employed the mass spectrometry technologies of D_2O-based protein turnover and concentration measurement to open new research avenues in the fields of cardiac function and aging in higher organisms.[9, 12, 13] These studies answer questions few if any other methods can conquer.

1.5 Recent D_2O-based Turnover Studies

Recent publications have shown the utility of D_2O labeling to investigate protein turnover in murine models and humans. Price et al. and Wang et al. have both shown protein turnover can be measure in human serum using D_2O labeling methods.[14, 15] These methods present a new way of understanding metabolic changes and biomarkers in diseased patients. Kim et al., Kasumov et al., and Lam et al. have applied D_2O turnover experiments to murine cardiac systems to study mitochondrial turnover and early stage heart failure.[13,12,16] Cardiac turnover studies have identified localization specific changes in cardiac mitochondrial turnover and new insights into proteostasis, metabolism, mitochondrial dynamics and calcium signaling in early stage isoproterenol-induced heart failure. Price et. al used D_2O labeling to identify key hepatic metabolism changes associated with longevity in calorie restricted (CR) mice.[9] Specifically, this study identified bulk protein turnover is significantly slowed in calorie restriction, suggesting increased catabolism rates are not associated with long term CR-induced longevity as previously hypothesized. Rather, calorie restriction may be associated with a higher degree of protein quality control and global regulation of protein synthesis.

Recent developments in turnover proteomics have opened a new door into biomedical exploration in both model systems and clinical settings. These measurements allow biomolecule turnover rates to be measured *in vivo* using stable isotope tracers, which cause few undesirable perturbations. Further, advents in precursor pool measurement have provided rapid tests to

contextualize stable isotope ratios into definitive biomolecule turnover rates. Turnover techniques have been effectively employed in the both cardiac failure and calorie restricted mice. Based on these studies we chose to kinetically interrogate ribosome protein quality control and global regulation of protein synthesis in CR. The ribosome regulates protein translation and is a large complex with complex proteostasis.

1.6 The Ribosome

The ribosome is an extremely costly, large ribonucleoprotein complex requiring hundreds of proteins to synthesize. Ribosome synthesis is controlled by the nutrient-sensing mTORC1 (mammalian target of rapamycin complex 1).[17] In nutrient replete conditions, mTORC1 contributes to ribosome biogenesis by initiating ribosomal protein and ribosomal ribonucleic acid (rRNA) transcription. 47S pre-rRNA is transcribed in the nucleolus and processed into 28S, 18S, and 5.8S rRNA. 5S rRNA is produced separately and ribosomal proteins are imported into the nucleolus after translation. Together the 40S and 60S subunits consist of 4 rRNA's, and ~80 ribosomal proteins and require about 200 helper proteins to be assembled and exported from the nucleus.

After assembly 40S and 60S ribosomes are shipped from nucleus to the cytoplasm or cytosolic membrane of the endoplasmic reticulum and begin translating messenger ribonucleic acid (mRNA). 40S and 60S ribosomes remain separate until elongation initiation factors recruit mRNA's from translation (see Figure 2). Following mRNA recruitment, 60S and 40S ribosomes form an 80s complex clamped onto mRNA. After 80s formation, transfer RNA (tRNA) charged with an amino acid enter the ribosome amino acyl (A) site. tRNAs contain 3 base pair sequences that are complementary to coding mRNA sequences. When a tRNA complimentary to the mRNA enters the A site, a peptide bond is made, linking the amino acid in the A site to an amino acid in

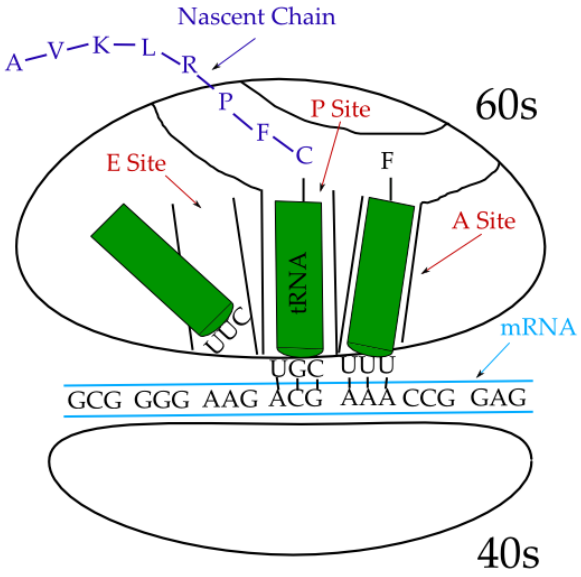

Figure 2: Basic 80s Ribosome Function

The 80s ribosome translates mRNA into protein. The eukaryotic ribosome consists of 2 subunits, the 40S and 60S, ~80 ribosomal proteins and 4 rRNA's. 40S and 60S subunits together with mRNA form the 80s subunit. The 80s subunit guides charged tRNAs to match mRNA sequences and deliver specific amino acids for protein assembly. After peptide bond formation the uncharged tRNA leaves the ribosome through the exit site.

the neighboring peptidyl (P) site. After peptide bond formation, the tRNA in the A site moves to the P site, and the covalent bond between the tRNA and the amino acid is broken. The discharged tRNA then leaves the ribosome through the exit (E) site. All mRNA precursor proteins must be translated through the ribosome to reach fruition, and the ribosome is conserved through all known species. Considering the critical role the ribosome plays in protein production and the major cost associated with ribosome synthesis, it is not surprising quality control mechanisms to maintain the ribosome have evolved.

Ribosome quality control has been categorized into two broad areas: 1. Total ribosome destruction through ribophagy 2. Rescue of stalled ribosomes through the ribosome quality control complex (RQC).[18, 19] Similar to autophagy, ribophagy involves the total engulfment of the 60S ribosome by an autophagosome followed by subsequent steps leading to lysosomal destruction. 60S ribosomes are protected from ribophagy by ubiquitination of RPL25. When RPL25 is

deubiquitinated the 60S ribosome is destroyed. The ribosome quality control complex removes the nascent chain from stalled ribosomes to help restore functionality. Ribophagy and ribosome quality control mechanisms provide explanation into total 60S ribosome homeostasis and quality control; however, additional studies suggest individual ribosomal subunits may be replaced without destruction of the entire ribosome.

Exchange of ribosomal components has been shown in prokaryotics, eukaryotics *in vitro* and *in vivo* in rapidly dividing *E. coli*. Pulk et al. showed chemically modified *E. coli* ribosomes exchange damaged proteins with undamaged proteins and regain activity *in vitro*.[20] Zinker et al. showed similar work in 80s yeast ribosomes after treatment with cycloheximide.[21] Additional work by Chen et al. using ^{15}N pulse-chase labeling, showed assembled ribosomes proteins turnover at different rates in rapidly dividing *E. coli*.[22] These studies provide strong preliminary evidence for individual ribosomal protein exchange without destruction of the entire ribosome. We aim to expand this work by investigating eukaryotic protein turnover in mouse liver. Eukaryotic ribosome synthesis is distinctly nuclear, adding a layer of physical separation and regulation as compared to prokaryotic cells. Additionally, slowly dividing tissues minimize protein dilution effects that occur in rapidly dividing cells.

To this end, we investigated mouse liver ribosomal protein turnover rates *in vivo* using stable isotope labeling techniques. To further understand the role protein quality control plays in ribosome homeostasis, we examined protein turnover under nutrient replete and 40% dietary restriction (DR). Ribosomal composition is known to change under nutrient stress.[23] Additionally, 40% calorie restriction slows bulk protein turnover and acts in part through mTOR regulation of ribosomal biogenesis.[9 24]

1.7 Calorie Restriction and Dietary Restriction

Calorie restriction (CR) is the most ubiquitous method for extending lifespan across many species.[25, 26, 27, 28] CR involves restricting calorie intake without decreasing essential nutrient intake. A true calorie restriction requires measuring mouse food intake and then reducing calories by a given percentage. Dietary restriction (DR) is similar, but does not measure mouse food intake before beginning food restrictions and does not replace lost vitamins and minerals. National Institutes of Health (NIH) have prescribed calorie restriction regimens for mice. Specifically the NIH-31 diet is used at 40% calorie restriction, a decrease from 5 grams to 3 grams of food per day.

Calorie restriction improves longevity and reduces disease occurrence. In many mouse genotypes, a 40% CR can result in a 40% increase in lifespan. CR also reduces occurrences of cancer, type 2 diabetes, and neurodegenerative disorders. Four major pathways have been implicated in the CR effect: the sirtuin pathway, the adenosine monophosphate-activated protein kinase pathway (AMPK) pathway, the insulin like growth factor (IGF-1)/insulin signaling pathway, and the mammalian target of rapamycin (mTOR) pathway.[29] We employed a 40% dietary restriction in mice based on NIH guidelines, but using a slightly different diet, to study effects on ribosome biogenesis and component replacement. Even after 40% DR, essential vitamins and minerals were still delivered at satisfactory concentrations. Ribosome biosynthesis is under mTOR control, suggesting large differences may be identified and eventually could be associated with DR phenotypes.

1.8 Experiment Summary

We employed kinetic proteomic and rRNA turnover techniques to better understand ribosomal component turnover in *ad libitum* (AL) fed and dietary restricted (DR) hepatic tissues (see Figure3). Dietary restriction was administered for 10 weeks prior to D_2O labeling. D_2O was

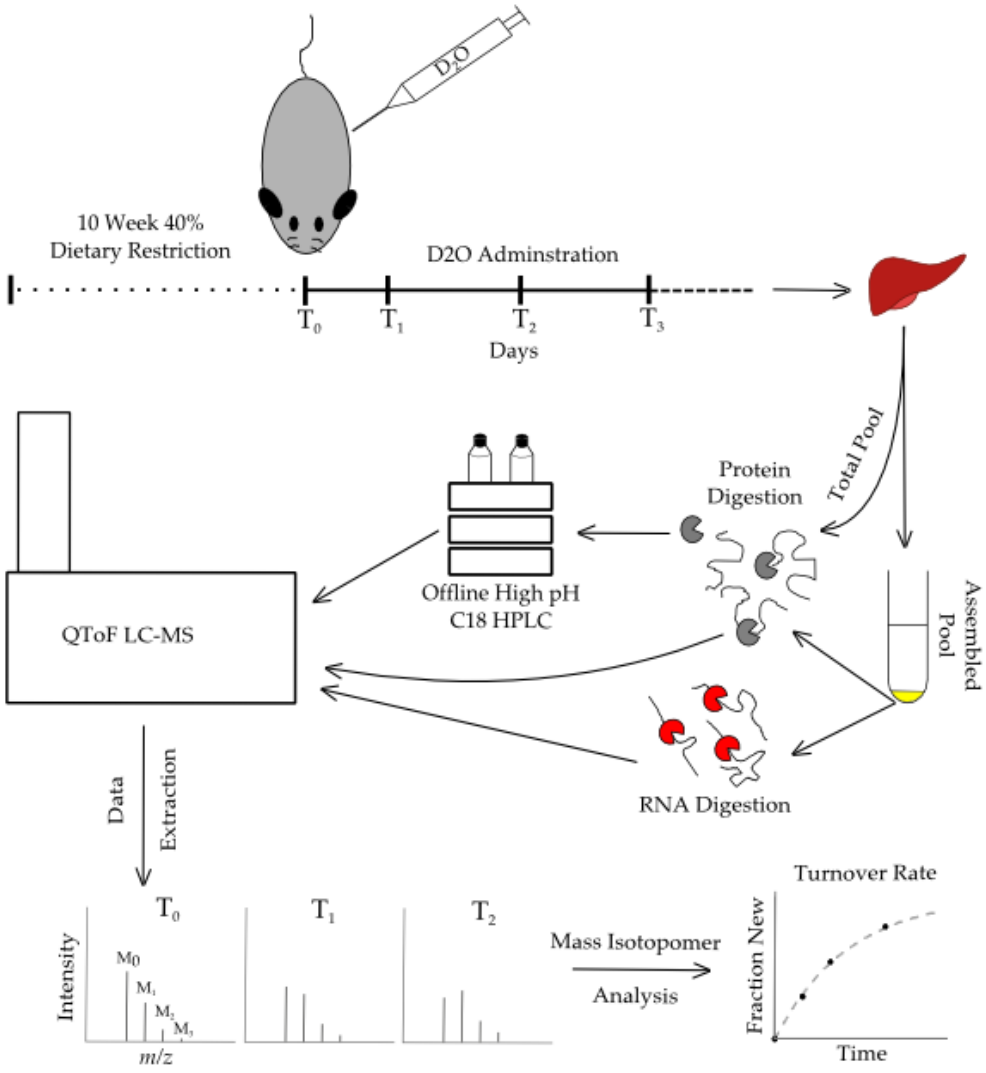

Figure 3: Experimental Design

Kinetic proteomics and rRNA analysis experimental workflow. Ribosomal protein turnover was measured using stable isotope labeling and mass spectrometry. Mice were dietary restricted for 10 weeks then labeled with D_2O continuously and sacrificed over a time course. Ribosome liver protein turnover was analyzed in whole lysate (total pool), and enrichment of ribosomes (assembled pool). rRNA turnover was also determined from the assembled pool. After mass spectrometry, data were analyzed using mass isotopomer distributions and turnover rate was calculated using first-order rate kinetics.

administered by intraperitoneal injection and drinking water to rapidly increase and maintain 5% D_2O *in vivo* enrichment throughout the duration of the experiment. Mice were sacrificed across a time course from zero (no D_2O administration) to thirty-two days. Ribosome kinetics were analyzed in both liver lysate and ribosomes purified through a sucrose cushion by mass spectrometry and mass isotopomer distribution analysis.

Kinetic analysis showed that ribosomal proteins are replaced at significantly different rates suggesting individual ribosomal proteins can be replaced without destruction of the entire ribosome. Additionally, rRNA measurements are consistent with bulk ribosomal protein turnover and provide a metric of ribophagy. Dietary restricted mice showed increases in ribosomal protein turnover compared to *ad libitum* fed mice. However, ribophagy as measured by rRNA turnover did not significantly change. This study provides insights into ribosome maintance in two different cellular states and provides a method to directly measure ribophagy at homeostasis *in vivo*.

Chapter 2: Materials and Methods

2.1 Mouse Handling

Mice were housed, dietary restricted, and metabolically labeled according to NIH-approved practices. Protocols were performed with permission from the Brigham Young University Institutional Animal Car and Use Committee. Ten Week old male C57BL/6 mice were obtained from Charles River Laboratories. For the duration of the experiment, mice were housed in an specific-pathogen-free (SPF) facility with 12 hour light/dark cycles. All mice were allowed one week on *ad libitum* fed diet to equilibrate with 3–4 mice per cage. After one week mice were separated and assigned to a 40% dietary restricted or *ad libitum* fed diet on Harlan 8604 food. Mouse weights were taken each week and weight homeostasis was obtained in *ad libitum* and dietary restricted mice. After 10 weeks of treatment, mice received a 5% body weight intraperitoneal sterile D_2O injection to immediately bring body water to 5% D_2O. Drinking water was supplemented to 8% D_2O to maintain 5% body water throughout the experiment. Mice were sacrificed in at least duplicate at time points 0 days (no D_2O injection), 0.375 days, 1 day, 2 days, 4 days, 8 days, 16 days, and 32 days. Sacrifice was performed using CO_2 asphyxiation followed by diaphragm puncture. Mice were immediately dissected, blood was extracted by cardiac

puncture for % D_2O analysis, and organs were flash frozen on blocks of solid CO_2. Tissues were stored at -80 °C.

2.2 Ribosomal Assembled Pool Enrichment

Separation of free ribosomal proteins and assembled ribosomes was performed using a modified procedure from Ingolia et al.[30] Frozen liver, 62–215mg, from time points 0, 1 day, 4 days, 8 days, and 16 days was homogenized in polysome buffer (20mM Tris/HCl, 150 mM NaCl, 5 mM $MgCl_2$, 1 mM Dithiothreitol, 1:100 dilution protease inhibitor cocktail (Sigma), and 1% Triton X-100) using a bead homogenizer: 30 seconds, 4 m/s, repeated 1–3 times depending on need. Lysate was placed into a new Eppendorf tube and clarified by centrifugation at 20,000g for 20 minutes at 4 °C. After clarification, sample was decanted then ~300 µL was passed through a 2.2mL sucrose cushion (1M sucrose, 20mM Tris/HCl, 150 mM NaCl, 5 mM $MgCl_2$, and 1 mM Dithiothreitol) for 12 hours at ~200,000g (40,600rpm) 4 °C using a ti-55 rotor on the Optima L-100XP Ultracentrifuge (Beckman Coulter). After centrifugation, sucrose was decanted and the ribosome pellet was suspended in 6M Guanidine/HCl, 100mM Tris/HCl pH 8.5.

2.3 Mass Spectrometry Sample Preparation

Ribosomal samples were prepared for mass spectrometry using modified filter-aided sample preparation. Briefly, protein was denatured in 6M Guanidine/HCl 100mM Tris/HCl (pH 8.5), cysteines were reduced using dithiothreitol and alkylated using iodoacetamide. Samples were placed on 500 µL 10kD or 30kD filters and washed 2–3 times on the filters using 6M Guanidine/HCl 100mM Tris/HCl pH 8.5. The guanidine solution was removed by two to three 25mM ammonium bicarbonate washes. Proteins were resuspended in 25 mM ammonium bicarbonate and digested overnight using Pierce MS-Grade Trypsin in a 1:50 (w:w) ratio or

minimum 0.1 μg or 0.5 μg of trypsin per sample. Trypsin digest was quenched using phenylmethane-sulfonylfluoride (PMSF) or centrifuging through above mentioned filters to remove tryspin. Samples were spun through filters, placed in mass spec vials, speed vacuumed to dry, and then suspended at ~1 μg/μL in 3% acetonitrile 0.1% formic acid.

Total pool ribosome samples were prepared from whole liver lysates using similar protocols. Liver was homogenized in a 100 mM ammonium bicarbonate solution with the protease inhibitor cocktail (Sigma) aiming for a final concentration of approximately 10 mg/ml protein concentration. Approximately 500 μg of protein was lysed in 6M Guanidine/HCl 100mM Tris/HCl and subject to similar filter-aided preparations and trypsin digestion as described above. After digestion, samples were spun through filters, speed vacuumed to dry, and resuspended in 10 mM LC-MS grade ammonium formate pH 9.5.

Samples were fractionated using high pH C_{18} high performance liquid chromatography (HPLC), which is orthogonal to low pH C_{18} chromatography. Fractionation was performed using the 1260 HPLC Infinity (Agilent) and the Gemini 50 x 2.00 mm C18 column with 3μm beads and 110 angstrom pore size. Peptides were eluted using a 10 mM ammonium formate pH 9.5 H_2O/acetonitrile gradient from 3% B to 60% B over 40 minutes flowing at 1 mL/min. Gradient A is 97% H_2O, 3% acetonitrile, 10mM ammonium formate pH 9.5. Gradient B is 10% H_2O, 90% acetonitrile, 10mM ammonium formate pH 9.5. 1 mL fractions were collected. 1 mL fractions were pooled into 8 fractions by pooling every 8^{th} fraction. For instance fractions 1, 9, 17, 25,… would be pooled into one fraction. Pooled fractions were speed vacuumed to dryness then suspended in 200 μL of 80% acetonitrile (to extract peptides but leave some salts) and decanted into a mass spectrometry vial. Samples were again speed vacuumed to dry and then suspended in 40 μL of 3% acetonitrile 0.1% formic acid for LC-MS analysis.

2.4 LC-MS Proteomics Acquisition

Protein identification and kinetic acquisition were performed on the Agilent 6530 Q-ToF mass spectrometer coupled to capillary and nanoflow Agilent 1260 HPLC using the chipcube nano-spray source. Peptides were eluted from the Agilent C18 Polaris chip at 300 nL/min using an H_2O-Acetonitrile gradient acidified to 0.1% Pierce LC-MS grade formic acid. Buffer A was 3% acetonitrile, 0.1% formic acid. Buffer B was 97% acetonitrile, 0.1% formic acid. The elution gradient is as follows: 0 minutes, 100% A; 0.1 minutes, 95% A; 27 minutes, 40% A; followed by high percentage B column washing and low percentage B equilibration. The Agilent 6530 Q-ToF mass spectrometer was run in 2 Ghz high dynamic range mode. Protein identification runs were performed in MSMS mode using collision induced dissociation with nitrogen gas. MS^1 and MS^2 data were collected at a maximum rate of 4 spectra/second with CID fragmentation on the top 10 most abundant precursors. Dynamic exclusion was set to 0.2 minutes. Kinetic acquisitions were performed in MS-only mode and collected at 1 spectra/second. MS only mode increases signal intensity, improves signal-to-noise, and gives more scan points per elution chromatogram greatly enhancing isotopomer analysis accuracy.

2.5 Peptide Identification

Peptide identifications were made using SpectrumMill then overlaid onto kinetic acquisitions. SpectrumMill searches were performed against the Uniprot Mouse database with MS^1 tolerance ±20ppm and a MS^2 tolerance ±50 ppm, cabomidomethylation (C) as a static modification, and pyroglutamic acid (n-term) and oxidation(M) as dynamic modifications.

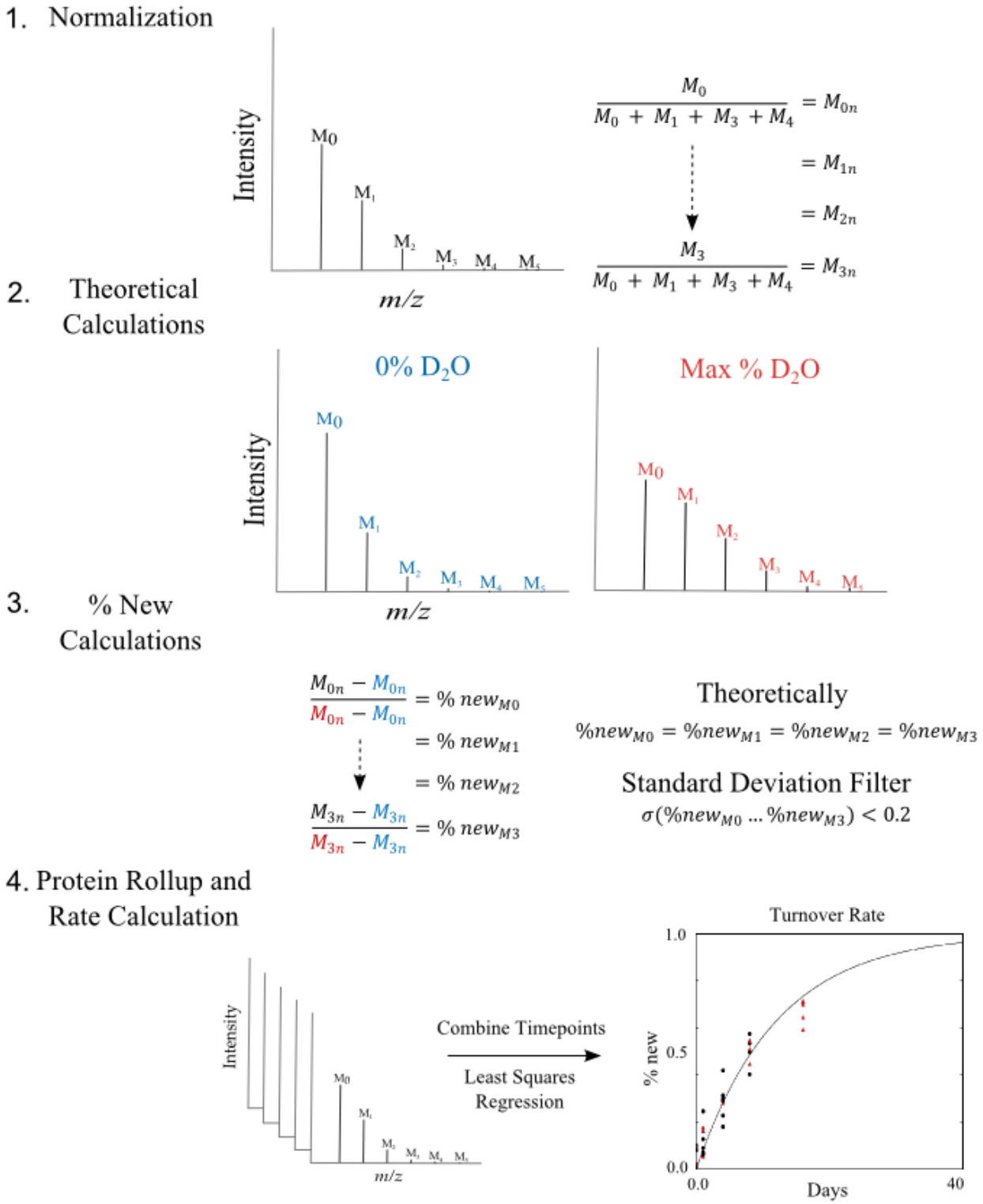

Figure 4: Mass Isotopomer Analysis Workflow

Data analysis workflow to determine turnover rate. 1. Mass spectral data must be normalized according to the number of isotopomer peaks included in the calculation. Number of isotopomer peaks to include is based on peptide *m/z*. 2. Theoretical calculations are made based on mouse body D_2O enrichment. % D_2O is a direct measure of the precusor pool allowing a theoretical maxium to be calculated based on D_2O incoporation into amino acids.

3. Normalized data and theoretical calculations are combined to determine % new peptide. % new peptide should be equal for all isotopomer peak normalized ratios. The standard deviation of % new peptide for the isotopomer peaks is used as a filter for high quality data. 4. Peptides are grouped into proteins and the median % new protein, based on M_0, is plotted along with a standard deviation. Data from multiple timepoints and biological replicates at the same timepoint are combined. A rate is fit based on first-order rate kinetics using a non-linear least squares regression.

Searches were performed using trypsin as a digestion enzyme allowing 2 missed cleavages. A second search with no specific enzyme was performed against a restricted library of identified proteins. Identified peptides were exported and used to calculate mass isotopomer distributions and extract peptide isotope patterns from MS-only acquisitions.

2.6 Mass Isotopomer and Kinetic Analysis

MassHunter software was used to extract peptide isotope patterns from MS-only acquisitions. MS-only isotopomer data was extracted based on peptide identification from MSMS acquisition using *m/z* (± 12 ppm) and retention time alignment (± 0.8 minutes). Data were then processed using in house python-based programs based upon previous publications by Price et al.[9] Briefly, isotope peaks M_0–M_4 were normalized then compared to theoretical calculations based on percentage D_2O enrichment to determine fraction deuterium enriched (new) peptide (see Figure 4). Theoretical calculations were determined using the eMASS algorithm and based on the number of possible deuterium incorporation sites per amino acid.[31] Theoretically, changes in abundance of each isotope peak M0–M_n can be used to determine percent new peptide; however, M_0–M_4 are the most abundant and give better results. A standard deviation of change was taken for M_0–M_4 (peptide mass above 2400 Daltons) or M_0–M_3 (peptide mass below 2400). If the percentage new peptide standard deviation exceeded 0.2, the data point was removed from downstream analysis. Additional filters were also applied to remove peptides with total relevant intensity below 20,000 counts and a retention time deviation greater than 0.4 minutes.

Peptide data were combined into proteins and fit according to first-order rate kinetics. M_0 % new data from the above mentioned peptides are combined and fit using a non-linear least squares regression based on first-order rate kinetic equations. Time point zero is forced to 0% new and is given a standard deviation of 0.05. A given protein's rate is only calculated when 3 or more time points have protein data.

Proteins were colored by turnover rate (red fastest, blue slowest) on a high resolution cryo-electron microscopy human ribosome structure by Khatter et al.[32]

2.7 rRNA Turnover Analysis

rRNA turnover analysis was performed as follows: ribosome pellets from the sucrose cushion centrifugation were resuspended in 6M Guanidine/HCl 100mM Tris/HCl pH 8.5. Appoximently half of this sample was subjected to RNA purification using the PureLink RNA Mini-Kit. The remaining rRNA was stored at -80 °C until RNase digestion. RNA was digested in 100mM ammonium bicarbonate 5 mM EDTA pH 7.5 overnight at room temperature with RNase A/T1 (Fisher). The digest was stored frozen until mass spectrometry analysis.

Mass spectrometry analysis was performed on the Agilent 6530 Q-ToF coupled to the Agilent 1260 capillary HPLC using the Jetstream ESI source. Nucleotides were desalted then eluted from a Zorbax SB-C18 150 x 0.5mm column with 5 μm resin using a 5mM ammonium acetate pH 5.0/MeOH gradient at 50 μL/min. The elution gradient is as follows: 0.0–0.30 min ,0.0% MeOH; 0.30–0.31 min, 0.0–0.2% MeOH; 0.31-0.45 min, 0.2–0.4% MeOH; 0.45–1.0 min, 0.4–1.5% MeOH followed by column washing at 90% MeOH. MS only and MSMS spectra were collected for analysis. Mass isotopomer extractions and calculations were performed as described above with a few modifications. MassHunter *m/z* mass accuracy filter was set to ± 20 ppm. Mass isotopomer calculations were performed on guanosine monophosphate using Isotopomer3.01

software based on 5 incorporated deuteriums. Only M_0 was used for % new analysis and errors are solely based on standard deviations from least squared fits to first-order rate kinetics. Data was fit using GraphPad Prism.

2.8 Quantitative Polymerase Chain Reaction

Quantitative polymerase chain reaction (qPCR) was performed using SBYR green on the Applied Biosytems 7500 instrument. Reverse transcription was performed with the iScript cDNA synthesis kit (Bio Rad) and SYBR green master mix (Bio-Rad). Primers: 18s rRNA forward(CTTAGAGGGACAAGTGGCG) reverse(ACGCTGAGCCAGTCAGTGTA); 16s Mitochondrial rRNA forward(CGAGGGTCCAACTGTCTCTT) reverse(GGTCACCCCAACC GAAATTT); vRNA forward(GCTGAGCGGTTACTTTGACA) reverse(GTCTCGAACCAA ACACTCATG); TATA forward(ACAGCCTTCCACCTTATGCT) reverse (GATTGCTGTA CTGAGGCTGC). qPCR instrument parameters were as follows: Stage 1 (1 cycle) 50 °C for 2 minutes; Stage 2 (1 cycle) 95 °C for 15 seconds; Stage 3 (30–45 cycles depending on need), 95 °C for 15 seconds, 59 °C for 1 minute. Melt curves to determine product purity and efficiency calculations were performed on all primer sets (supplemental data). qPCR primer efficiency was calculated using Real-time PCR Miner 4.1.[33] Relative concentrations were calculated using method by Pfaffl, which corrects for differences in primer efficency.[34]

2.9 Statistical Analysis

Statistical analysis was performed in Microsoft Excel, Graph Pad Prism and the JMP software package. Graphs were made in Microsoft Excel. Graph Pad Prism was used to fit the rRNA turnover rates to a first-order rate kinetic and calculate 95% confidence intervals. JMP was used to calculate *p*-values and 95% confidence intervals for protein turnover data comparisons. R^2

adjust values were calculated in JMP according to linear fits. R^2 values were calculated in Microsoft Excel.

2.10 Mouse Ribosome Compared to *E. coli* Turnover

Proteins with sequence homology from an *E. coli* ribosome protein turnover study were compared to wild-type turnover rates in mouse liver (see Supplementary Figure 3). Rates for *E. coli* ribosomal proteins turnover and mouse protein turnover differed significantly in range; therefore, within each species rates were normalized against the fastest turnover ribosomal protein measured. This normalization effectively rank orders ribosomal proteins by turnover rate allowing a more direct comparison. Homology was determined by searching identified mouse ribosomal proteins against the *E. coli* database using NCBI protein BLAST. Mouse ribosomal proteins with any sequence homology to *E. coli* ribosomal proteins were included in the analysis. Scores were associated with the probability of a given match happening by random chance in a database of given size. A score of 1 indicates a high likelihood of the match occurring by random chance. Scores do not have a finite range, but the lowest NCBI grouping is below 40 and the highest above 200. R^2 was calculated using Microsoft Excel.

2.11 Yeast Eukaryotic Versus Mitochondrial Ribosome Absolute Concentrations

Eukaryotic versus mitochondrial ribosome concentration estimations from this study were compared to absolute protein concentration measurements by Ghemmhagami et al. A median absolute concentration value was taken from 107 eukaryotic ribosomal proteins and 62 mitochondrial proteins. The median value was used to represent the given ribosome concentration.

Chapter 3: Ribosome Turnover in Mouse Liver

Kinetic proteomics and rRNA turnover analysis show that the protein components of eukaryotic ribosomes in mouse liver turnover at different rates. Mice were labeled with and maintained at 5% D_2O body water and sacrificed over a time course ranging from 0 to 32 days. After sacrifice hepatic ribosomes were isolated from free pool ribosomal proteins through a sucrose cushion using ultracentrifugation and then analyzed by liquid chromatography mass spectrometry (LC-MS) to determine protein turnover rates. Increases in fraction of deuterated protein/RNA were used as a metric of biomolecule turnover. Ribosome turnover data from sucrose cushion isolated ribosomes will be referred to as the assembled pool (proteins are assembled into the ribosome) and ribosome turnover data from the whole lysate will be referred to as the total pool (see Figure 3).

3.1 Ribosomal Proteins in the Assembled Structure Turnover at Different Rates

Assembled pool ribosomal proteins turnover at different rates (see Figure 5). Assembled pool ribosomal protein (n=58) turnover ranged from 3.7% to 15.8% new protein per day with an 9.3% average rate and 2.0% rate standard deviation. Most ribosomal protein grouped close to the average, suggesting degradation by ribophagy, however, four proteins were more than two standard deviations above the average: RPL19, RPL34, RPS27-like, and RPL10. And one proteins was more than two standard deviations below the average: RPLP1. Though average ribosomal protein turnover rate is probably a good metric of ribosome turnover, we measured rRNA turnover in the assembled pool to directly quantify ribophagy. Comparing ribophagy rates directly to protein turnover better identifies ribosomal proteins that may be individually exchanged after ribosome incorporation.

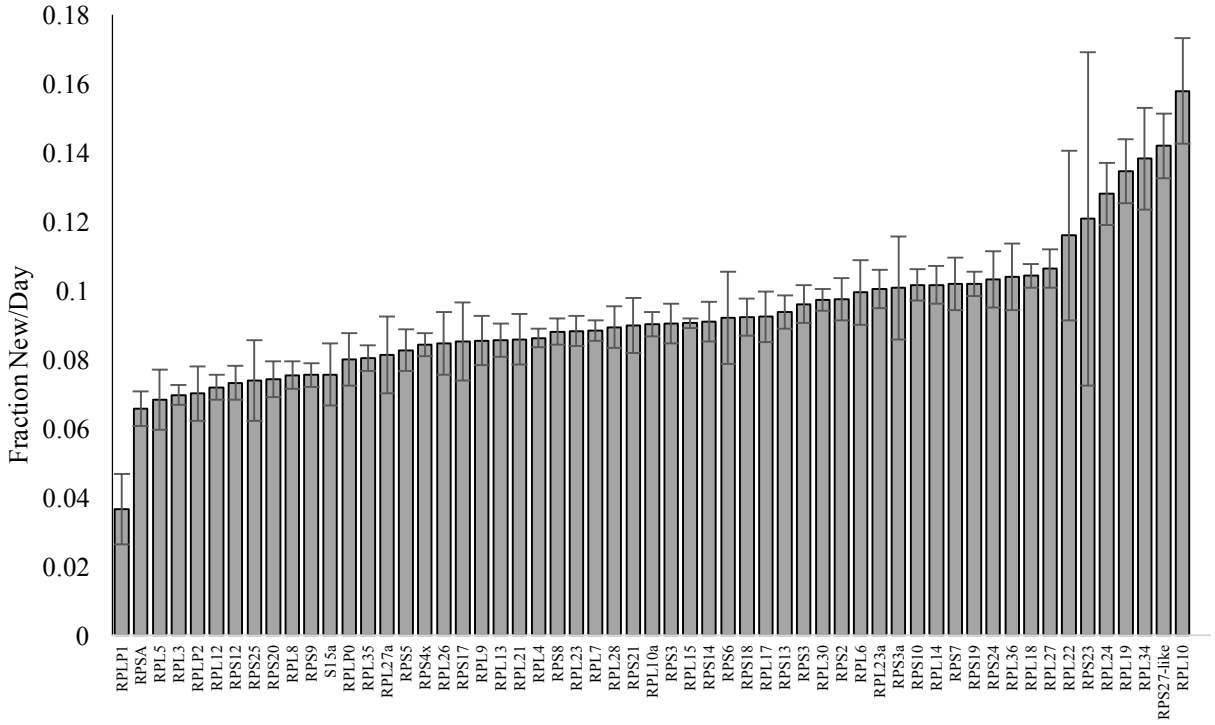

Figure 5: Ribosomal Proteins Turnover at Different Rates

Protein turnover was measured in assembled ribosomal proteins from *ad libitum* fed mouse liver. Rates vary from 3.7% to 15.8% suggesting some ribosomal proteins are can be replaced after ribosome assembly. Error bars are standard deviations from first order rate fits.

Comparing ribophagy to protein turnover identified more ribosomal proteins that may be exchanged within the ribosome (see Figures 6–7). rRNA turnover showed ribophagy occurs at 8.8% new ribosome per day (95% confidence interval (CI) from 7.3% to 10.4%) in mouse liver, which is similar to the 9.3% average ribosomal protein turnover rate. Five proteins were shown to be more than one standard deviation above the upper limits of the ribophagy 95% confidence interval suggesting these proteins may be individually replaced in assembled ribosomes: RPL19, RPL34, RPS27-like, RPL10, and RPL24. These proteins may be extracted and destroyed instead of recycled into the free ribosomal protein pool or alternatively free pool turnover may be very fast and assembled to free pool turnover is rapid (Figure 11). Two ribosomal proteins, RPLP0 and

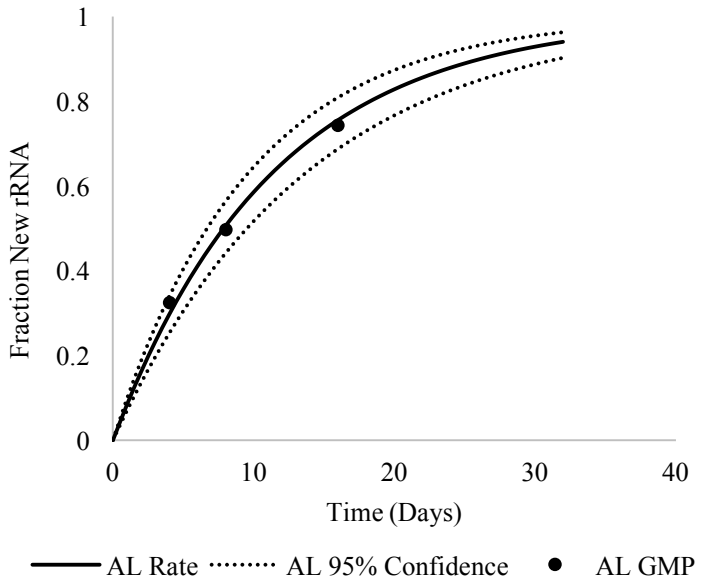

Figure 6: rRNA Turnover as a Metric of Ribophagy

rRNA turnover was measured from the assembled ribosomal pool of three mice. Isotope incorporation into Guanosine monophosphate (GMP) turnover rate was fit with first order rate kinetics. Ribophagy rate is 8.8% new/day 95% CI from 7.3% to 10.4% new rRNA per day.

RPSA, were more than one standard deviation below the ribophagy 95% CI lower bound. This data suggests RPSA and RPLP0 may be removed and eventually incorporated into new ribosomes before ribophagy destruction or alternatively free pool turnover is very slow, but exchange between free pool and assembled pool is very fast. Though assembled pool ribosomal protein turnover compared to ribophagy provides compelling evidence ribosome incorporated proteins can be exchanged individually, these diverse ribosomal protein turnover rates may be caused by biases from free pool ribosomal protein turnover. To address this concern, we performed turnover proteomics on total pool (assembled pool + free pool) ribosomal proteins to identify large changes in ribosomal protein turnover between pools that could bias assembled pool turnover rates.

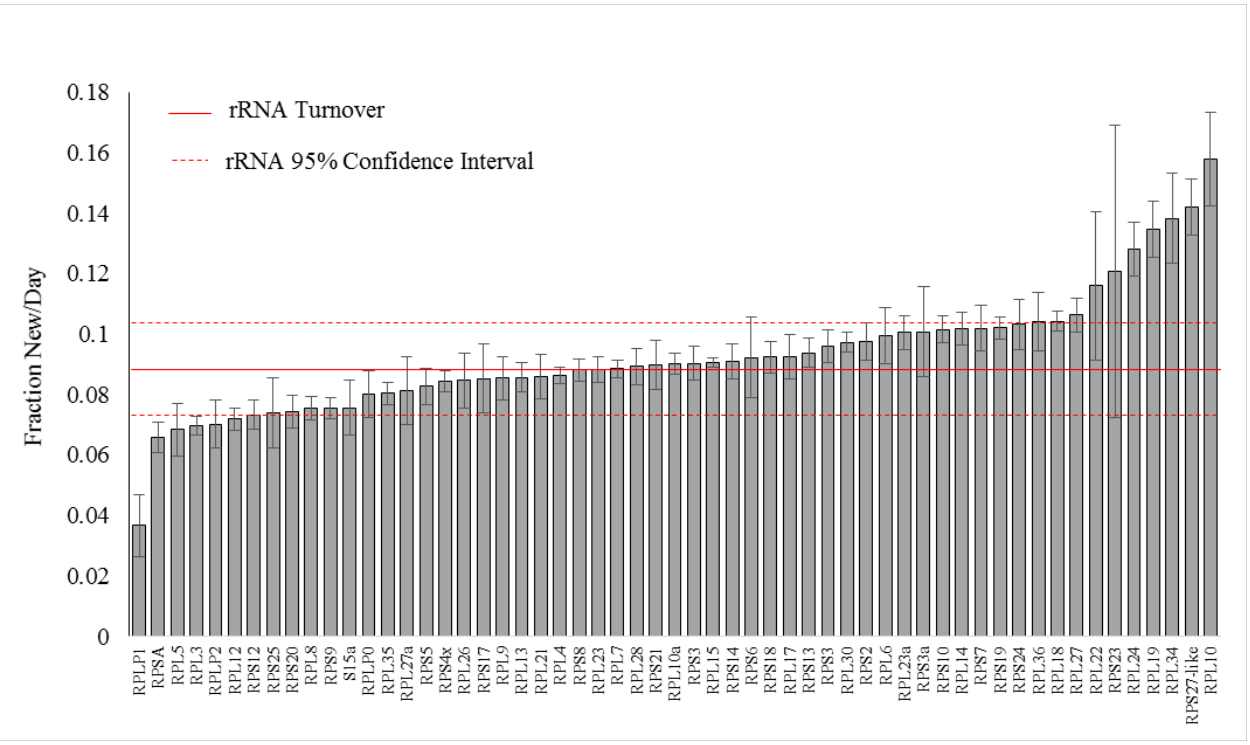

Figure 7: Ribophagy Rate Identifies Exchangeable Proteins

Assembled pool protein turnover rates were plotted with the rRNA turnover rate to determine whose turnover is significantly above or below ribophagy rates. Comparison identifies 7 ribosomal proteins that do not fall within the rRNA 95% confidence interval: RPL10, RPS27-like, RPL34, RPL19, RPL24, RPSA, and RPLP1

Turnover data show many proteins have subtle but statistically significant changes between the assembled pool and the total pool (see figure 8a). Little or no change in total pool turnover suggests two possibilities: 1. Most ribosome proteins bulk concentration exists in the ribosomal pool. 2. The free pool and ribosomal pool turnover at similar rates. Diversity in total pool and assembled pool turnover rates suggests within ribosome protein turnover is not purely an artifact of free ribosomal pool turnover. Linear regression analysis shows a possible significant difference between AL assembled and whole pools (fit line slope = 0.64, *p*-value = 0.0006, 95% CI from 0.296 to 1.000). Many proteins show a potential for within ribosome exchange based on total versus free pool turnover data, but excluding proteins whose assembled protein turnover was within ribophagy rate: RPLP0 and RPL10 seem most likely. A brief study of RPLP0 rate fit showed a bimodal distribution in % new protein, suggesting RPLP0 has splice variants or a post-

translational modification. Two RPLP0 peptides were identified and are from the same splice variant. RPLP0 is acetylated at A2 and phosphorylated at S101 in humans.[35, 36] We identified the peptide containing S101, but did not identify the phosphorylation. However, these bimodal rates could still be explained by S101 phosphorylation. Further analysis of RPLP0 turnover is required to understand this result. We also looked at the structure position of RPL10 in the 80s human cryo-electron microscopy structure to qualitatively interrogate the possibility of RPL10 exchange based on location.

RPL10 is located in the mRNA binding pocket and is very solvent exposed especially when the 60S subunit is free from the 40S subunit (see Figure 9). Additionally, RPL10 plays important roles in ribosome quality control, motion, and 80s formation. Solvent exposure without any protein segments buried deep within the ribosome increases the likelihood that RPL10 can be exchanged. The other fastest turnover proteins, RPL19, RPL24, RPL35, and RPS27 are also fairly solvent exposed. However, quantitative comparison of turnover to protein binding will require surface area analysis. To further understand ribosomal protein turnover, we perturbed a known regulator of ribosome biogenesis, mTOR, through 40% dietary restriction.

3.2 Ribosomal Protein Turnover Changes Significantly in Dietary Restriction

Assembled ribosomal protein turnover increases in dietary restriction. Ribosome homeostasis is controlled in part by the nutrient sensing mTOR complex 1 (mTORC1). We altered mTORC1 response through a 40% dietary restriction in mice to better understand ribosome homeostasis and to identify proteins that may exchange after ribosome turnover. We employed the same kinetic proteomic and rRNA turnover techniques used on the wild-type fed mice. Linear regression shows a potential increase in DR protein turnover (fit line slope = 0.66, p-value = 0.011, 95% CI from 0.28 to 1.04) with a protein turnover range from 4.5% to 23.6% new protein. (see

A

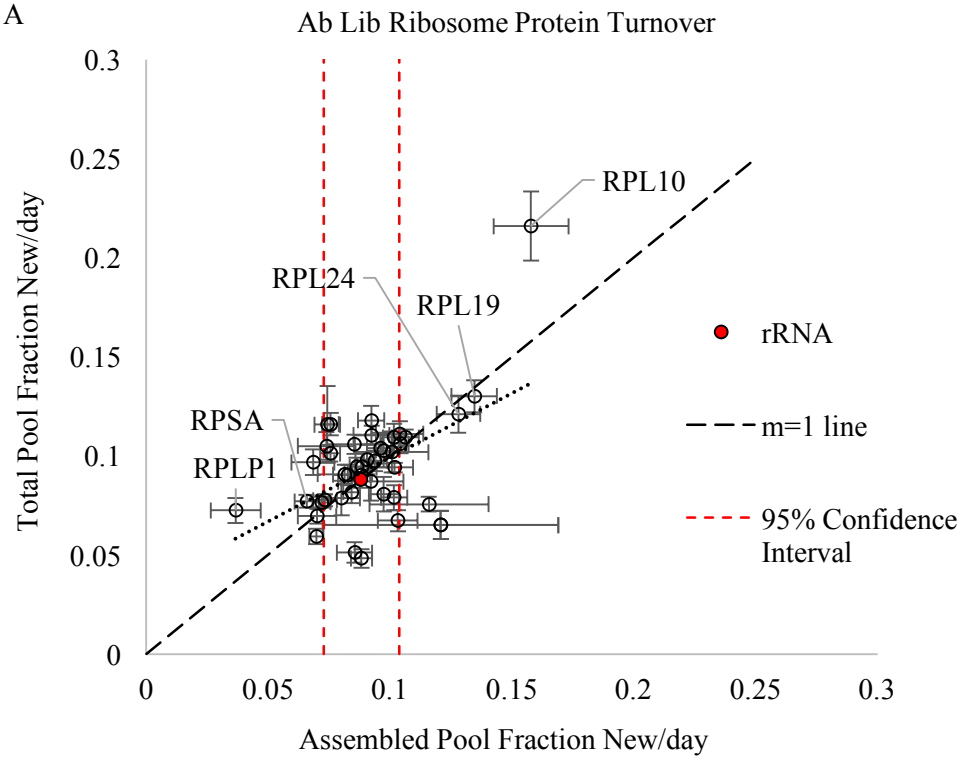
Ab Lib Ribosome Protein Turnover
Total Pool Fraction New/day
Assembled Pool Fraction New/day
0.3
0.25
0.2
0.15
0.1
0.05
0
0
0.05
0.1
0.15
0.2
0.25
0.3
RPL10
RPL24
RPL19
RPSA
RPLP1
rRNA
m=1 line
95% Confidence Interval

C

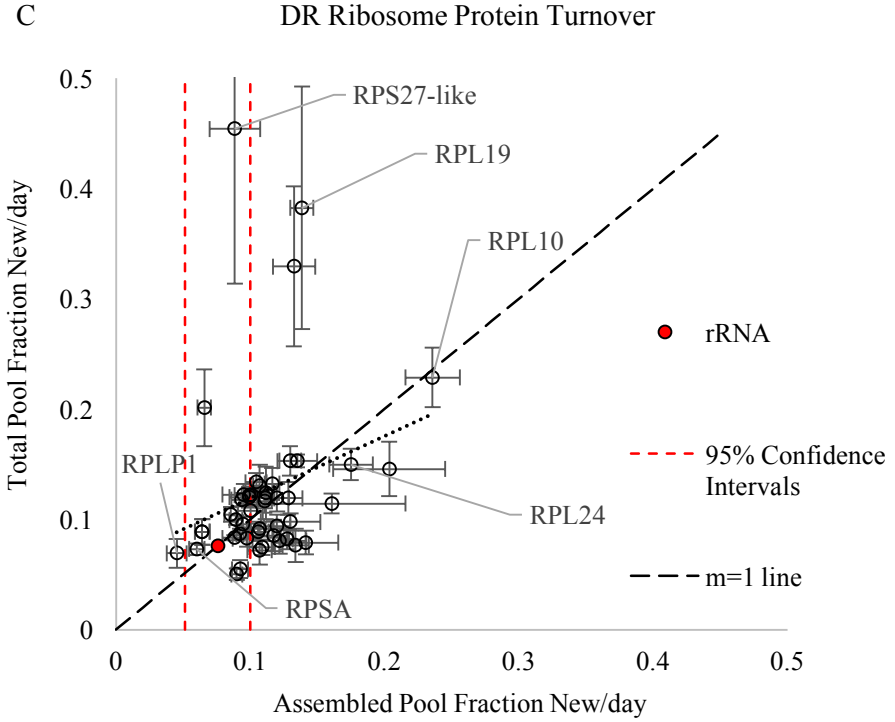
DR Ribosome Protein Turnover
Total Pool Fraction New/day
Assembled Pool Fraction New/day
0.5
0.4
0.3
0.2
0.1
0
0
0.1
0.2
0.3
0.4
0.5
RPS27-like
RPL19
RPL10
RPLP1
RPL24
RPSA
rRNA
95% Confidence Intervals
m=1 line

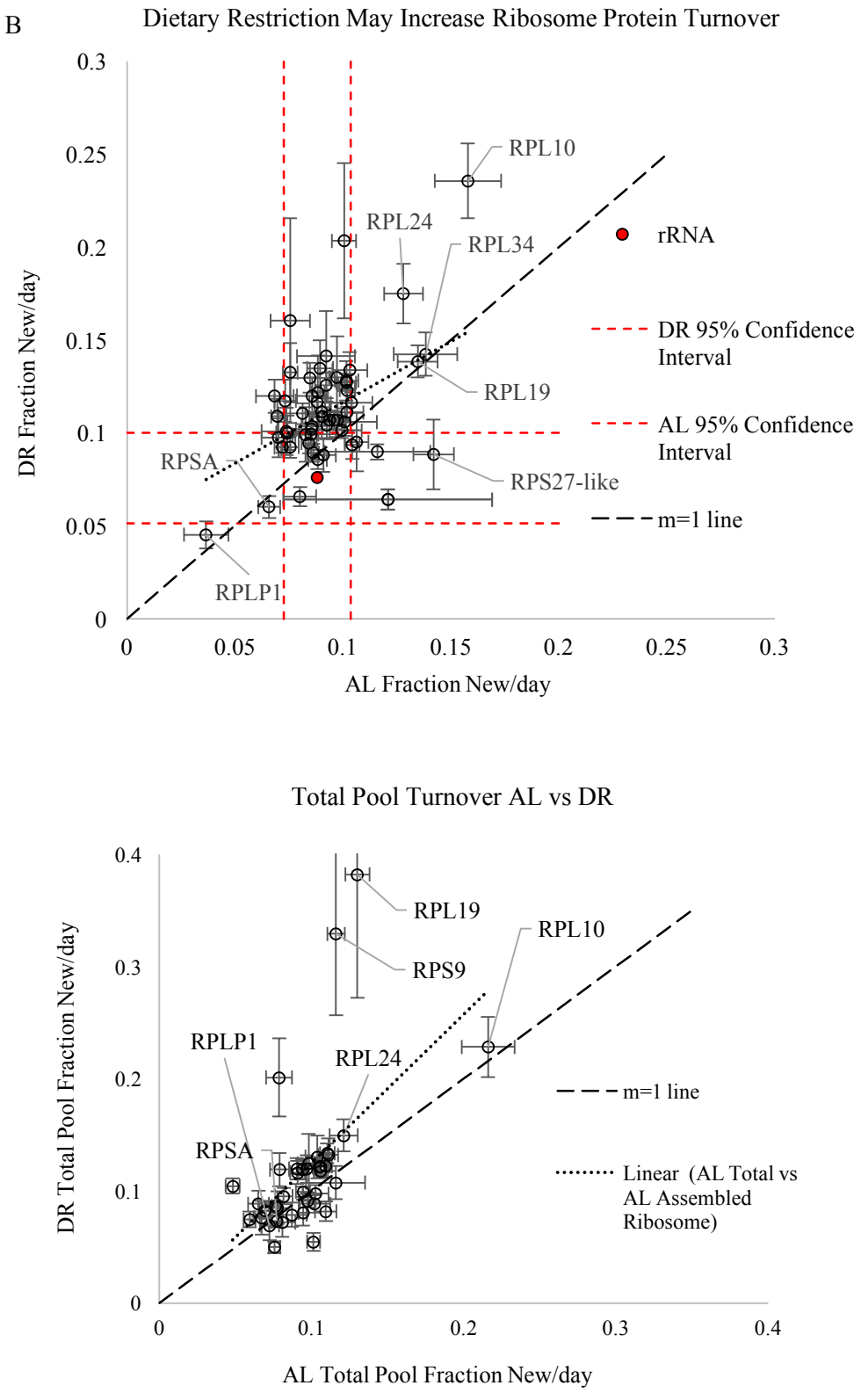

Figure 8: Ribosome Proteins Turnover Can Differ in Assembled vs Total Pool

AL and DR rRNA turnover rates (AL: 8.8% and DR: 7.6%) and 95% rRNA turnover confidence intervals (AL: 7.3% to 10.4% and CR: 5.1% to 10.0%) are plotted on relevant graphs A. AL ribosomal Proteins turnover at different rates in assembled vs total pools. R^2 adjusted = 0.23, fit line slope=0.64, *p*-value=0.0006, 95% CI from 0.296 to 1.000 B. DR increases assembled ribosome pool turnover. Correlation is higher than AL assembled pool versus total pool, R^2 adjusted = 0.17, fit line slope = 0.66, *p*-value = 0.011, 95% CI from 0.28 to 1.04 C. DR total less similar to DR assembled pool R^2 adjusted = 0.04, but outliers likely skew the correlation. There is no significant difference between pools. Fit line slope = 0.56, *p*-value = 0.10, 95% CI from -0.10 to 1.23. D. DR total pool similar to AL total pool. R^2 adjusted = 0.28, fit line slope = 1.31, *p*-value = 0.0003, 95% CI from -0.64 to 1.98.

Figures 8b-c) An adjusted R^2 of 0.17 shows a weak correlation still exists between DR and AL assembled ribosomes. Importantly, RPL10 showed a significant shift in turnover from 15.8% to 23.6% new protein per day.

Considering a bulk increase in ribosomal protein turnover we hypothesized one of three possibilities: 1. DR ribophagy increased. 2. Ribosome concentration decreased, 3. Free pool turnover increased. Surprisingly, ribophagy if anything slowed in DR samples: 7.6% new ribosomes/day (95% CI from 5.1% to 10.0%, see Figure 9). Another possibility is that DR ribosome concentration decreases, but turnover rate was maintained causing faster protein replacement. Again surprisingly, 40S rRNA PCR showed no decrease in ribosome concentration (1.11 fold increase in CR standard deviation = 0.09). Lastly, a total increase in ribosomal protein turnover could explain the increased ribosomal protein turnover rates associated with assembled ribosomes in DR. DR total pool turnover measurements when compared to DR assembled pool measurements showed no significant difference (Fit line slope = 0.56, *p*-value = 0.10, 95% CI from -0.10 to 1.23). DR ribosomal protein turnover increase is primarily attributed to changes in assembled pool kinetics because DR total pool and AL total pool are very similar (fit line slope = 1.31, *p*-value = 0.0003, 95% CI from -0.64 to 1.98, R^2 adjusted 0.28, see Figure 8D).

RPL10 turnover rate in DR assembled and DR total pools (Assembled: 23.6%, Total: 22.8%) was much more similar than expected when compared to the stark RPL10 turnover difference in AL pools (Assembled: 15.8%, Total: 21.6%). Diversity in assembled versus total

pool turnover rate suggests a two-pool kinetic where ribosomal proteins have diverse rates in distinct pools.

3.3 Ribosomal Protein Two-Pool Kinetic

Ribosomal proteins exist in at least one of two conditions: the free pool or the assembled pool (see Figure 11). The free pool is loosely defined as all ribosomal proteins that are not assembled into a ribosome; therefore, ribosomal proteins only escape the free pool when incorporated into the ribosome. Many studies have shown ribosomal protein insertion into the ribosome occurs in the nucleolus prior to ribosome transport into the cytoplasm.[37] After a life time of translation, 60s ribosomes are known to be destroyed as an assembled ribophagy mechanism. However, this mechanism does not explain the diverse ribosomal protein rates measured by this study. As such we hypothesize post ribosome assembly mechanisms exist to allow active and/or passive insertion of ribosome protein constituents. In this way these large and expensive biological machines can be maintained and repaired while maximizing the cellular economy.

The measured turnover rate and ribophagy rate in DR show RPL10 is very likely replaced throughout ribosome lifespan (see figure 11). RPL10 turnover rate changes significantly in the AL assembled versus total pools from 15.8% to 21.6% (see Figure 8a). However, in DR RPL10 turnover rate changes from 23.6% to 22.8% (see Figure 8c). Therefore, total pool turnover increases by 1.2% and assembled pool turnover increases by 7.8%. Ribophagy, as measured by rRNA turnover, does not change significantly, so only 1.2% of the RPL10 increase in turnover in the assembled pool can be attributed to changes in total pool turnover. The remaining DR induced increase in RPL10 turnover is likely due to a change in equilibrium between free and assembled pools.

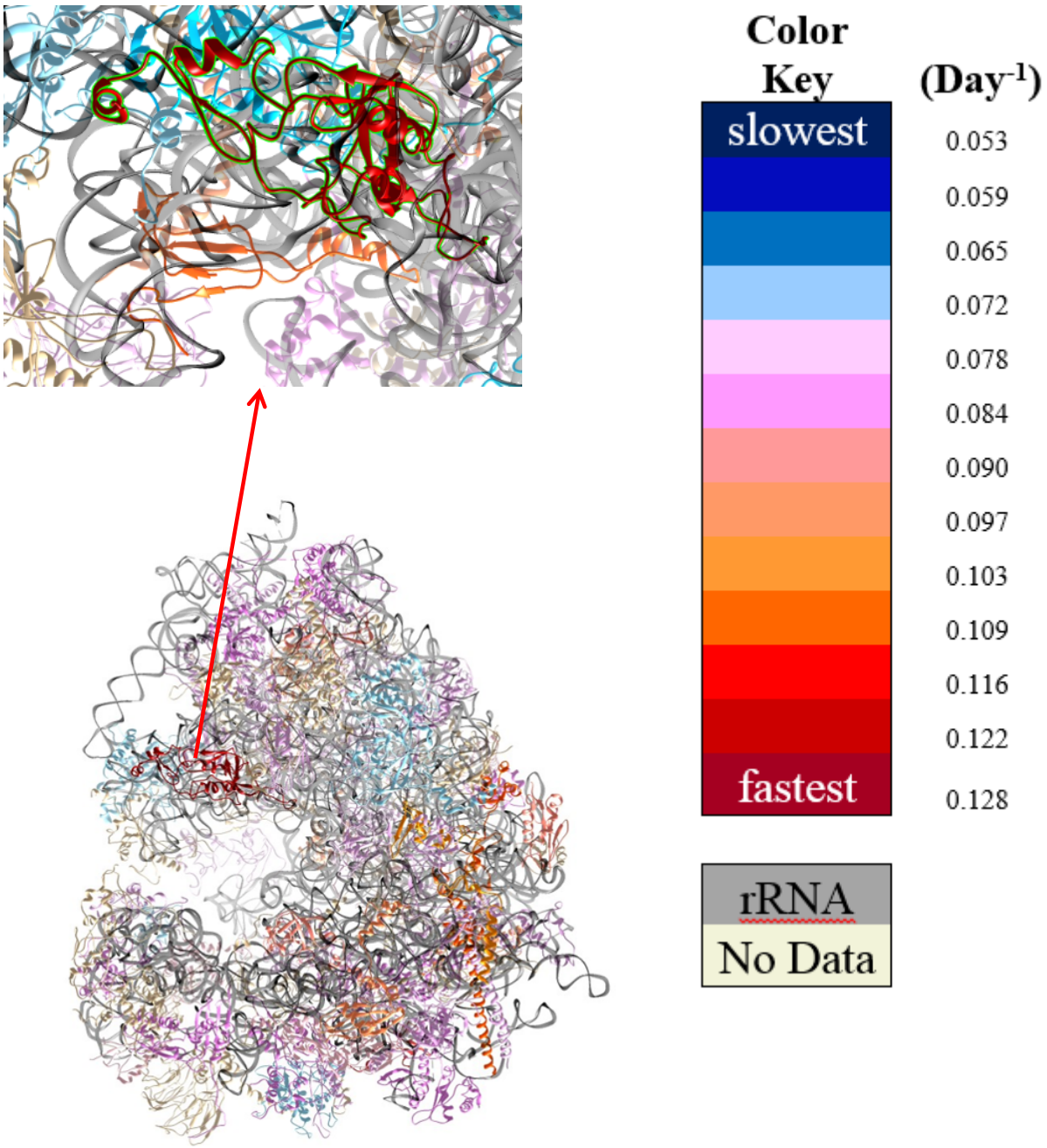

Figure 9: RPL10 Location Makes Exchange More Likely

Ribosomal proteins were colored according to rate (red fastest and blue slowest) on the human 80s ribosome to allow qualitative comparison of rate and location. The fastest turnover protein, RPL10, is located in the mRNA binding pocket and is not buried deeply in the ribosome.

Chapter 4: Discussion

4.1 Measuring Ribosome Homeostasis

Mouse hepatic ribosome turnover kinetics show ribosomal protein turnover differs significantly, suggesting some ribosomal proteins may be replaced during ribosome lifespan. Ribosomal protein turnover has been previously measured in *E. coli* and also showed ribosomal proteins turnover at different rates.[22] However, no significant correlation was found between protein homologs in mouse liver and *E. coli* (supplemental figure). Differences between prokaryotic and eukaryotic ribosomes including changes in ribosome structure, extra-ribosomal function as well as the rapidity of *E. coli* cell division could account for these disparities.

Comparison of ribosomal protein turnover rates to ribophagy rates allowed the identification of proteins that turnover significantly faster or slower than total ribosome turnover. Previous studies made rRNA turnover measurements *ex vivo* and *in vivo* including in humans using heavy labeled glucose.[38,39,40,41] Because previous studies were not performed in liver tissues, a direct comparison of riboghay rates cannot be made, however, rRNA turnover rates were still similar. In a study by Defoiche *et al. in vivo* rRNA turnover in $CD3^-$ cells from a patient with chronic lymphocytic leukemia were 11.6% new/day during pulse and 5.8% new/day during chase, and rRNA turnover in young cultured mouse fibroblasts was 9.2% new/day. However cultured young mouse fibroblasts were dividing every 30 hours, which suggests minimum percent new ribosome should be closer to 50%.[41] This discrepancy maybe accounted by incorrect precursor pool measurements or challenges putting new ribosomes in the context of total ribosomes.

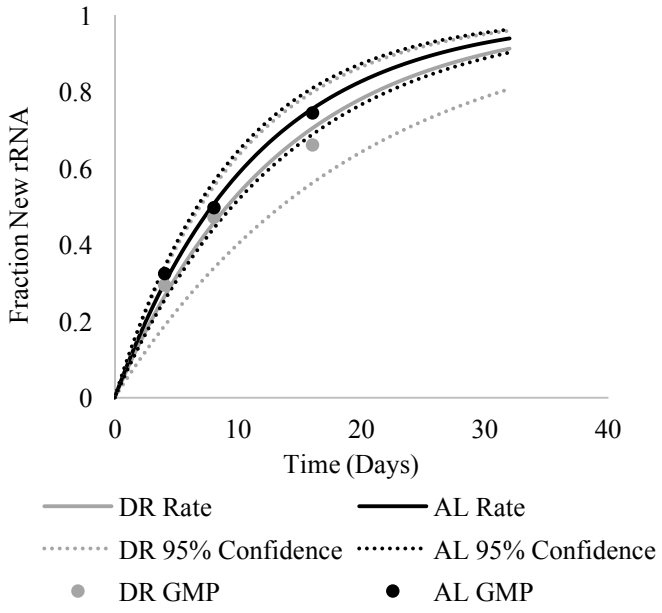

Figure 10: rRNA Turnover is Similar in AL and DR

rRNA turnover rates were calculated based on GMP deuterium enrichment. rRNA was extracted from the assembled ribosome fraction. Data were fit to a first order kinetic and 95% confidence intervals were calculated AL: 8.8% new rRNA/day, 95% CI from 7.3% to 10.4% and DR: 7.8% new rRNA/day, 95% CI from 5.1% to 10.0%.

At homeostasis assembled ribosome rRNA turnover is a direct measure of ribophagy. Ribosomal protein may be replaced throughout ribosome lifespan, but there is no evidence indicating rRNA is replaced during ribosome lifespan. Furthermore, no evidence suggests a free rRNA pool of significant size, and strong evidence suggests at least some misprocessed rRNAs are targeted for exosome destruction.[42] Additionally, rRNA was extracted from ribosomes after sucrose cushion enrichment, which selects for high density particles. High density particles may include pre-40S and pre-60S complexes, but based on ribosome turnover rates these complexes are likely in low stoichiometry compared to mature ribosomes. Lastly, eukaryotic ribosome turnover may be biased by other high density RNA containing protein complexes especially the mitochondrial ribosome. To discern the effect of mitochondrial rRNA on eukaryotic rRNA turnover, we employed qPCR and RNA turnover measurement on ribosome purifications with and without Triton X-100 on AL mouse liver. Expecting Triton X-100 to increase mitochondrial

permeability and increase mitochondrial ribosome enrichments. Data showed a ten-fold increase in mitochondrial rRNA as compared to eukaryotic rRNA did not have a significant effect on rRNA turnover (see supplemental figure 2). Stoichiometrically the eukaryotic ribosome has ~2.7 time more base pairs than the mitochondrial ribosome. Lastly, using absolute quantitation data in yeast from Gheammhagami et al. we estimate eukaryotic ribosome to mitochondrial concentration ratio to be approximately 14.5:1 respectively, meaning total rRNA base-pair stoichiometry is approximately 39.2:1 eukaryotic to mitochondrial. Though this metric does not quantitatively translate to mouse liver, this data strenthgns our results that mitochondrial rRNA is less abundant than eukaryotic rRNA.

We performed turnover proteomics on total pool ribosomal proteins to show differences in assembled pool ribosomal protein turnover was not simply an artifact of total pool turnover. Differences in total and assembled pool turnover is not surprising considering the many known extra-ribosomal functions of ribosomal proteins. Further free subunits generally turnover more rapidly than assembled complexes. Diversity in protein turnover rates between total pools and assembly pools lead to the development of a two-pool kinetic model for ribosome turnover. The two-pool kinetic model places ribosomal proteins into a free pool or assembled pool. Where the free pool is all proteins that are not ribosome bound. Ribosomal proteins move from the free pool to the assembled pool through ribosomal assembly processes or by exchange after ribosome assembly. Turnover data from total pool and assembled pools strongly suggests at least some ribosomal proteins are exchanged after ribosome assembly.

Seven ribosomal proteins turnover differs significantly from ribophagy turnover rates. RPL10, RPL24, RPL19, RPS27, and RPL35 turnover more rapidly than the measure ribophagy rate. Fast turnover suggests ribosomal proteins are in rapid exchange with a fast turnover free

pool or ribosomal proteins are immediately destroyed after removal from the ribosome. RPL10 appears to exchange quickly with a faster turnover pool. RPL19 and RPL24 turnover about the same rate in total and assembled pools. Interestingly, when the 80S ribosome is assembled, RPL24, RPL19 and RPL35 all span between the 40S and 60S ribosome suggesting proteins key to 80S ribosome assembly are continually replaced. Ribosomal proteins that are key to ribosomal function maybe replaced more often as a mechanism of ribosome quality control and repair. RPLP1 and RPSA turnover more slowly than the measured ribophagy rate. Slower turnover suggests rapid exchange with a slow turnover free pool or these proteins are escaping ribophagy and being assembled into new ribosomes. Unexpectedly, RPLP1 turnovers over more rapidly in the total pool but as mentioned previously, RPLP1 has a bimodal rate distribution suggesting post translational modification is playing a role in regulating RPLP1 turnover and may manipulate in ribosome function or structure.

4.2 Slight Changes in Diet May Alter Dietary Restriction Effects

Previous calorie restriction studies by Price et al. and Karunadharma et al. show decreases or no change in CR total pool mouse hepatic ribosomal protein turnover. [9, 24] Our study data shows an increase in ribosomal protein turnover in the assembled pool, but similar results in the total pools. However, global turnover proteomics data (data not shown) does not show the same DR turnover slowing expected based on previous studies. The same C57BL/6 mice were used in all studies, however, a few keys differences between studies exist. Age: Price et al. used 18-month-old mice, Karunadharma et al. had two groups of mice 3-month-old mice and 25-month-old mice, and the current study used 3-month-old mice. Gender: Karunadharma et al. used female mice, whereas Price et al. and the current study used male mice. Importantly, the same general trends in protein turnover were seen between Price et al. and Karunadharma et al. older mice. Diet: Price

et al. and Karunadharma et al. used 40% calorie restriction, whereas this study used a 40% dietary restriction. However, both Price et al. and this study fed the same amount of food to calorie/dietary restricted mice. Price et al. used the NIH-31 gold standard diet for calorie restriction. Karunadharma et al. used a diet nutritionally similar to NIH-31, Harlan Teklad diet #TD.99366. We used the Harlan 8604 diet, which contains about 6% more protein and 6% less carbohydrate than the NIH-31 diet. Fat, carbohydrate, and protein sources also differed between diets.

Despite unexpected shifts in global homeostasis, our data show slight changes in nutrient intake may significantly alter ribosome homeostasis. However, connections between ribosome homeostasis and longevity and aging cannot yet be directly drawn from this study.

4.3 RPL10 Probably Exchanges after Ribosome Formation

Ribosomal protein L10 (RPL10) probably exchanges throughout ribosome lifespan. RPL10 turnover rates are significantly faster than ribophagy rates in *ad libitum* (AL) and dietary restricted (DR) mice. In AL mice RPL10 turnover is slower in the assembled pool than the total pool suggesting a two-pool kinetic (see Figure 11). In DR RPL10 assembled and total pool turnover are much closer to the AL total pool rate. However, ribophagy does not increase, suggesting RPL10 exchange rate between assembled pool to the free pool has increased. RPL10 assembled pool turnover increase in DR is not necessarily linear, but shows exchange is likely occurring between free and assembled ribosome pools. Further explanation of RPL10 function from previous studies strengthens the RPL10 exchange hypothesis.

Previous studies show RPL10 may be likely to exchange during ribosome lifespan. RPL10 is one of few ribosomal proteins that is incorporated into the ribosome after pre-60S export into the cytoplasm.[43] Cytoplasmic incorporation suggests that RPL10 active incorporation machinery exists in the cytoplasm, or RPL10 may be exchanged through passive mechanisms as has been

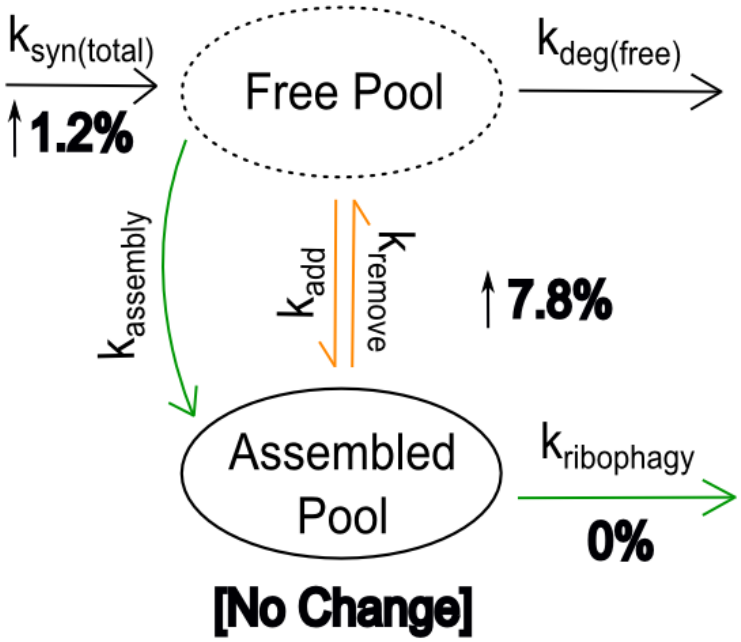

Figure 11: A Two-Pool Kinetic Model to Describe RPL10 Turnover Change in DR

$k_{syn(total)}$ represents the total measured synthesis. $k_{deg(free)}$ represents free pool degradation and was not directly calculated in this experiment. $k_{assembly}$ represents every new ribosome assembled and $k_{ribophagy}$ represents every ribosome destroyed and is measured by rRNA turnover. At homeostasis $k_{assembly} = k_{ribophagy}$. k_{add} and k_{remove} represent exchange of ribosomal proteins in the assembled pool. Exchange is partially measured by assembled pool turnover, but this measurement is biased by free pool turnover. DR increases RPL10 turnover by 1.2% in the total pool, but 7.8% in the assembled pool. Ribophagy does not functionally change.

shown previously *in vitro*.[21] RPL10 is located in the top of the mRNA binding pocket and has no regions that are deeply buried within the ribosome suggesting replacement can occur without disrupting ribosome structure.[32] Prior to 80s formation RPL10 quality control checks the 60S ribosome for functionality.[44] Newly synthesized subunits also require RPL10 to remove the NMD3P nuclear export adaptor before 80s formation can occur.[45] During translation RPL10 plays a major role in ribosome rotation, which is required for successful protein translation.[46] When translation has ended and the 80s ribosome dissociates, RPL10 is solvent exposed and possibly ready for exchange. Any significant damage to RPL10 would require exchange to maintain 60S ribosome functionality and ability to translate mRNA. Without RPL10 replacement, the ribosome would become useless and would have to be degraded.

Considering the crucial role RPL10 plays in ribosome function, the ribosome turnover data which suggest high rates of RPL10 replacement, the cytoplasmic incorporation of RPL10 into the ribosome, and RPL10 solvent exposure in the 60S ribosome, we propose RPL10 can be exchanged from the free 60S subunit *in vivo*. This exchange improves cellular efficiency by repairing the very costly 60S ribosome without total destruction. Further experiments targeting RPL10 and checking passive exchange rates will further solidify RPL10 exchange after ribosome assembly and RPL10 exchange restoring 60S ribosome functionality.

Chapter 5: Future Directions and Conclusions

5.1 Perform Calorie Restriction using Standardized NIH Diet

Comparing ribosome turnover from mice calorie restricted according to National Institutes of Health (NIH) gold standards will determine if subtle changes in diet change CR homeostasis. Using the same experimental tests, we will compare ribosomal homeostasis in the current study to calorie restricted mice fed the NIH-31 diet. The NIH-31 diet is the gold standard diet for calorie restriction studies. This comparison will serve three major purposes: 1. The comparison will confirm this study was performed correctly. 2. Ribosomal turnover changes can be more directly compared to longevity phenotypes. 3. Small changes in diet will be shown to have significant consequences on ribosome and cellular homeostasis.

5.2 Determine Eukaryotic Ribosomal protein K_d *In Vitro*

Measuring ribosomal component exchange *in vitro* will allow basic K_d to be estimated for ribosomal proteins. *In vitro* ribosomal protein K_d's for the assembled complex can be determined using tandem affinity purification (TAP)-tagged ribosomes, heavy isotope labeling, and mass spectrometry. Briefly, TAP-tagged ribosome will be purified from lysate using TAP affinity beads

and extracted. Ribosome bound beads will be placed in heavy labeled yeast lysate and allowed to incubate. Portions of beads will be extracted throughout the experiment and prepared for mass spectrometry. Throughout the time course, passively transported heavy isotope labeled ribosomal proteins will be exchanged into label free bead bound ribosomes. Rates of passive ribosomal protein exchange into assembled ribosomes will be measured using mass spectrometry. A similar experiment by Polk et al. was performed on damaged prokaryotic ribosomes *in vitro*.[20] This study showed damaged ribosomes can exchange components with undamaged ribosomes and regain function. Measuring *in vitro* eukaryotic ribosomal protein exchange will add to current knowledge in at least two important ways: 1. *In vitro* K_d values can be used in combination with *in vivo* turnover values to model ribosomal component exchange and the two pool kinetic model. 2. Comparing K_d values with protein turnover rates will aide in identifying potential active ribosomal component exchange *in vivo*. Simply, if the protein turnover rate is high, but K_d is low the given ribosomal protein may require active exchange.

5.3 Ribosomal Protein Surface Binding Analysis

Use solved ribosome structures to estimate ribosomal protein binding energy based on intra-ribosomal interactions. The energy associated with these protein-protein interactions will allow calculation of K_{eq}, which is equivalent to K_d at equilibrium. Theoretically, making the K_{eq} measurement, the K_d measurement, and the turnover rate measurement will provide complimentary data proving individual components of the ribosome can be exchanged *in vivo* (see Figure 11).

5.4 Conclusions

Using kinetic turnover analysis of ribosomal proteins and rRNA, we have shown ribosomal proteins are replaced at different rates *in vivo*. Differences between assembled and total pool protein turnover suggest individual ribosomal protein components can be replaced without ribosome destruction. It is likely that some ribosomal proteins, including RPL10, are made and destroyed without ever being assembled into a ribosome. This is not surprising considering ribosomal proteins are known to have extra-ribosomal functions and free protein subunits are generally destroyed more rapidly than assembled complexes. Based on assembled pool, total pool, and ribophagy turnover rates, we found that RPL10 likely exchanges throughout ribosome lifespan. Modeling RPL10 exchange we postulate a model in which ribosomal proteins exchange between an assembled pool and free pool. This model likely applies to many ribosomal proteins. Comparing DR and AL, RPL10 turnover rates shows RPL10 likely exchanges after incorporation into 60S ribosomes. These turnover data are consistent with known RPL10 functions and assembly mechanism and suggests that RPL10 is may be replaced to restore ribosome function.

References

1. Waterlow, J. C., *Protein turnover*. CABI: 2006.
2. Bennet, W.; GAN-GAISANO, M.; Haymond, M., Tritium and 14C isotope effects using tracers of leucine and alpha-ketoisocaproate. *European journal of clinical investigation* **1993,** *23* (6), 350-355.
3. Tarver, H.; Schmidt, C. L., RADIOACTIVE SULFUR STUDIES I. SYNTHESIS OF METHIONINE. II. CONVERSION OF METHIONINE SULFUR TO TAURINE SULFUR IN DOGS AND RATS. III. DISTRIBUTION OF SULFUR IN THE PROTEINS OF ANIMALS FED SULFUR OR METHIONINE. IV. EXPERIMENTS IN VITRO WITH SULFUR AND HYDROGEN SULFIDE. *Journal of Biological Chemistry* **1942,** *146* (1), 69-84.
4. Dietschy, J. M.; Spady, D. K., Measurement of rates of cholesterol synthesis using tritiated water. *Journal of lipid research* **1984,** *25* (13), 1469-1476.
5. Klyde, B. J.; Hirsch, J., Isotopic labeling of DNA in rat adipose tissue: evidence for proliferating cells associated with mature adipocytes. *Journal of lipid research* **1979,** *20* (6), 691-704.
6. Price, J. C.; Guan, S.; Burlingame, A.; Prusiner, S. B.; Ghaemmaghami, S., Analysis of proteome dynamics in the mouse brain. *Proceedings of the National Academy of Sciences* **2010,** *107* (32), 14508-14513.
7. Hellerstein, M.; Neese, R., Mass isotopomer distribution analysis: a technique for measuring biosynthesis and turnover of polymers. *American Journal of Physiology-Endocrinology And Metabolism* **1992,** *263* (5), E988-1001.
8. de Meer, K.; Roef, M. J.; Kulik, W.; Jakobs, C., In vivo research with stable isotopes in biochemistry, nutrition and clinical medicine: An overview. *Isot. Environ. Health Stud.* **1999,** *35* (1-2), 19-37.
9. Price, J. C.; Khambatta, C. F.; Li, K. W.; Bruss, M. D.; Shankaran, M.; Dalidd, M.; Floreani, N. A.; Roberts, L. S.; Turner, S. M.; Holmes, W. E., The effect of long term calorie restriction on in vivo hepatic proteostatis: a novel combination of dynamic and quantitative proteomics. *Molecular & Cellular Proteomics* **2012,** *11* (12), 1801-1814.
10. Doherty, M. K.; Whitehead, C.; McCormack, H.; Gaskell, S. J.; Beynon, R. J., Proteome dynamics in complex organisms: using stable isotopes to monitor individual protein turnover rates. *Proteomics* **2005,** *5* (2), 522-533.
11. Hsieh, E. J.; Shulman, N. J.; Dai, D.-F.; Vincow, E. S.; Karunadharma, P. P.; Pallanck, L.; Rabinovitch, P. S.; MacCoss, M. J., Topograph, a software platform for precursor enrichment corrected global protein turnover measurements. *Molecular & Cellular Proteomics* **2012,** *11* (11), 1468-1474.
12. Kasumov, T.; Dabkowski, E. R.; Shekar, K. C.; Li, L.; Ribeiro, R. F.; Walsh, K.; Previs, S. F.; Sadygov, R. G.; Willard, B.; Stanley, W. C., Assessment of cardiac proteome dynamics with heavy water: slower protein synthesis rates in interfibrillar than subsarcolemmal mitochondria. *American Journal of Physiology-Heart and Circulatory Physiology* **2013,** *304* (9), H1201-H1214.
13. Kim, T.-Y.; Wang, D.; Kim, A. K.; Lau, E.; Lin, A. J.; Liem, D. A.; Zhang, J.; Zong, N. C.; Lam, M. P.; Ping, P., Metabolic labeling reveals proteome dynamics of mouse mitochondria. *Molecular & Cellular Proteomics* **2012,** *11* (12), 1586-1594.
14. Price, J. C.; Holmes, W. E.; Li, K. W.; Floreani, N. A.; Neese, R. A.; Turner, S. M.; Hellerstein, M. K., Measurement of human plasma proteome dynamics with 2 H 2 O and liquid chromatography tandem mass spectrometry. *Analytical biochemistry* **2012,** *420* (1), 73-83.
15. Wang, D.; Liem, D. A.; Lau, E.; Ng, D.; Bleakley, B. J.; Cadeiras, M.; Deng, M. C.; Lam, M. P.; Ping, P., Characterization of human plasma proteome dynamics using deuterium oxide. *PROTEOMICS-Clinical Applications* **2014,** *8* (7-8), 610-619.
16. Lam, M. P.; Wang, D.; Lau, E.; Liem, D. A.; Kim, A. K.; Ng, D. C.; Liang, X.; Bleakley, B. J.; Liu, C.; Tabaraki, J. D., Protein kinetic signatures of the remodeling heart following isoproterenol stimulation. *The Journal of clinical investigation* **2014,** *124* (4), 1734.
17. Mayer, C.; Grummt, I., Ribosome biogenesis and cell growth: mTOR coordinates transcription by all three classes of nuclear RNA polymerases. *Oncogene* **2006,** *25* (48), 6384-6391.

18. Hinnebusch, A. G., Active destruction of defective ribosomes by a ubiquitin ligase involved in DNA repair. *Genes Dev.* **2009,** *23* (8), 891-895.
19. Brandman, O.; Stewart-Ornstein, J.; Wong, D.; Larson, A.; Williams, C. C.; Li, G.-W.; Zhou, S.; King, D.; Shen, P. S.; Weibezahn, J., A ribosome-bound quality control complex triggers degradation of nascent peptides and signals translation stress. *Cell* **2012,** *151* (5), 1042-1054.
20. Pulk, A.; Liiv, A.; Peil, L.; Maiväli, Ü.; Nierhaus, K.; Remme, J., Ribosome reactivation by replacement of damaged proteins. *Molecular microbiology* **2010,** *75* (4), 801-814.
21. Zinker, S.; Warner, J., The ribosomal proteins of Saccharomyces cerevisiae. Phosphorylated and exchangeable proteins. *Journal of Biological Chemistry* **1976,** *251* (6), 1799-1807.
22. Chen, S. S.; Sperling, E.; Silverman, J. M.; Davis, J. H.; Williamson, J. R., Measuring the dynamics of E. coli ribosome biogenesis using pulse-labeling and quantitative mass spectrometry. *Molecular Biosystems* **2012,** *8* (12), 3325-3334.
23. Garcia-Marcos, A.; Sánchez, S. A.; Parada, P.; Eid, J.; Jameson, D. M.; Remacha, M.; Gratton, E.; Ballesta, J. P., Yeast ribosomal stalk heterogeneity in vivo shown by two-photon FCS and molecular brightness analysis. *Biophysical journal* **2008,** *94* (7), 2884-2890.
24. Karunadharma, P. P.; Basisty, N.; Dai, D. F.; Chiao, Y. A.; Quarles, E. K.; Hsieh, E. J.; Crispin, D.; Bielas, J. H.; Ericson, N. G.; Beyer, R. P., Subacute calorie restriction and rapamycin discordantly alter mouse liver proteome homeostasis and reverse aging effects. *Aging cell* **2015**.
25. Houthoofd, K.; Vanfleteren, J. R., The longevity effect of dietary restriction in Caenorhabditis elegans. *Experimental gerontology* **2006,** *41* (10), 1026-1031.
26. Partridge, L.; Piper, M. D.; Mair, W., Dietary restriction in Drosophila. *Mechanisms of ageing and development* **2005,** *126* (9), 938-950.
27. Weindruch, R.; Walford, R. L.; Fligiel, S.; Guthrie, D., The retardation of aging in mice by dietary restriction: longevity, cancer, immunity and lifetime energy intake. *J Nutr* **1986,** *116* (4), 641-54.
28. Colman, R. J.; Beasley, T. M.; Kemnitz, J. W.; Johnson, S. C.; Weindruch, R.; Anderson, R. M., Caloric restriction reduces age-related and all-cause mortality in rhesus monkeys. *Nature communications* **2014,** *5*.
29. Speakman, J. R.; Mitchell, S. E., Caloric restriction. *Molecular aspects of medicine* **2011,** *32* (3), 159-221.
30. Ingolia, N. T.; Brar, G. A.; Rouskin, S.; McGeachy, A. M.; Weissman, J. S., The ribosome profiling strategy for monitoring translation in vivo by deep sequencing of ribosome-protected mRNA fragments. *Nature protocols* **2012,** *7* (8), 1534-1550.
31. Rockwood, A. L.; Haimi, P., Efficient calculation of accurate masses of isotopic peaks. *Journal of the American Society for Mass Spectrometry* **2006,** *17* (3), 415-419.
32. Khatter, H.; Myasnikov, A. G.; Natchiar, S. K.; Klaholz, B. P., Structure of the human 80S ribosome. *Nature* **2015**.
33. Zhao, S.; Fernald, R. D., Comprehensive algorithm for quantitative real-time polymerase chain reaction. *Journal of computational biology* **2005,** *12* (8), 1047-1064.
34. Pfaffl, M. W., A new mathematical model for relative quantification in real-time RT–PCR. *Nucleic Acids Res.* **2001,** *29* (9), e45-e45.
35. Desiderio, D. M., Identification and characterization of phosphorylated proteins in the human pituitary. *Proteomics* **2004,** *4*, 587-598.
36. Gauci, S.; Helbig, A. O.; Slijper, M.; Krijgsveld, J.; Heck, A. J.; Mohammed, S., Lys-N and trypsin cover complementary parts of the phosphoproteome in a refined SCX-based approach. *Analytical chemistry* **2009,** *81* (11), 4493-4501.
37. Venema, J.; Tollervey, D., Ribosome synthesis in Saccharomyces cerevisiae. *Annual review of genetics* **1999,** *33* (1), 261-311.
38. Gillery, P.; Georges, N.; Wegrowski, J.; Randoux, A.; Borel, J.-P., Protein synthesis in collagen lattice-cultured fibroblasts is controlled at the ribosomal level. *FEBS letters* **1995,** *357* (3), 287-289.

39. Defoiche, J.; Zhang, Y.; Lagneaux, L.; Pettengell, R.; Hegedus, A.; Willems, L.; Macallan, D. C., Measurement of ribosomal RNA turnover in vivo by use of deuterium-labeled glucose. *Clinical chemistry* **2009,** *55* (10), 1824-1833.
40. Yi, X.; Tesmer, V. M.; Savre-Train, I.; Shay, J. W.; Wright, W. E., Both transcriptional and posttranscriptional mechanisms regulate human telomerase template RNA levels. *Molecular and cellular biology* **1999,** *19* (6), 3989-3997.
41. Halle, J.; Müller, S.; Simm, A.; Adam, G., Copy number, epigenetic state and expression of the rRNA genes in young and senescent rat embryo fibroblasts. *European journal of cell biology* **1997,** *74* (3), 281-288.
42. Allmang, C.; Mitchell, P.; Petfalski, E.; Tollervey, D., Degradation of ribosomal RNA precursors by the exosome. *Nucleic Acids Res.* **2000,** *28* (8), 1684-1691.
43. West, M.; Hedges, J. B.; Chen, A.; Johnson, A. W., Defining the order in which Nmd3p and Rpl10p load onto nascent 60S ribosomal subunits. *Molecular and cellular biology* **2005,** *25* (9), 3802-3813.
44. Bussiere, C.; Hashem, Y.; Arora, S.; Frank, J.; Johnson, A. W., Integrity of the P-site is probed during maturation of the 60S ribosomal subunit. *The Journal of cell biology* **2012,** *197* (6), 747-759.
45. Hedges, J.; West, M.; Johnson, A. W., Release of the export adapter, Nmd3p, from the 60S ribosomal subunit requires Rpl10p and the cytoplasmic GTPase Lsg1p. *The EMBO journal* **2005,** *24* (3), 567-579.
46. Sulima, S. O.; Gülay, S. P.; Anjos, M.; Patchett, S.; Meskauskas, A.; Johnson, A. W.; Dinman, J. D., Eukaryotic rpL10 drives ribosomal rotation. *Nucleic Acids Res.* **2014,** *42* (3), 2049-2063.

Supplemental Figures

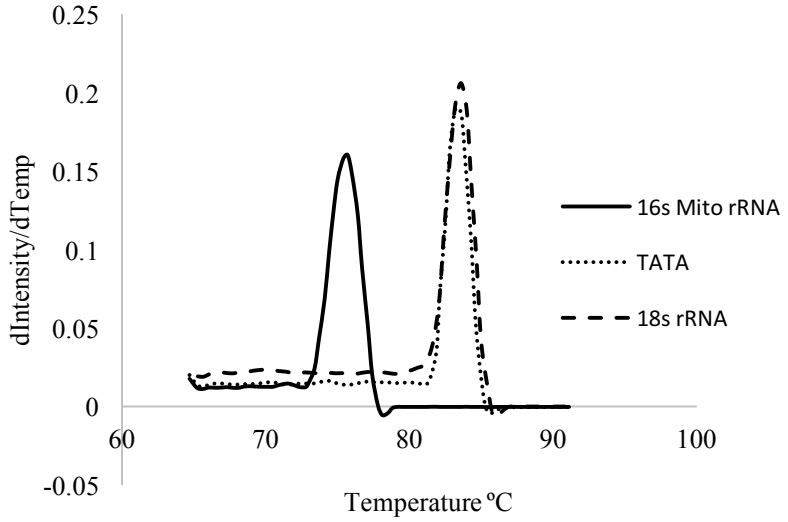

Supplemental Figure 1: qPCR primer melt curves

qPCR product melt curves from 16s mitochondrial rRNA, TATA Box binding protein rRNA, and 18s rRNA have a single signal as shown by slope derivative versus temperature.

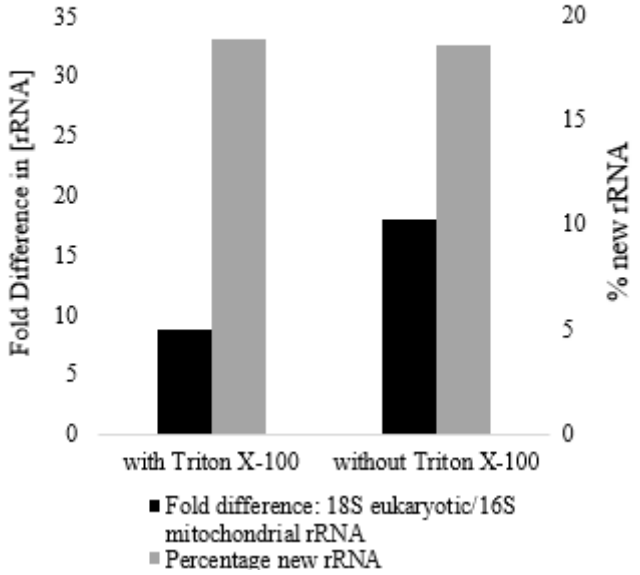

Supplemental Figure 2: *Ad libitum* rRNA turnover rate is not affected by changes in 16S mitochondrial rRNA concentration.

Mouse liver from time point 4 days was homogenized with and without Triton X-100 to determine how increased background RNA affects rRNA turnover rates after sucrose cushion ultracentrifuation. Triton X-100 should increase lysis efficiency by permeabilizing organelle membranes. qPCR was performed 18S rRNA and 16S

mitochondrial rRNA to show Triton X-100 extraction was effective. Turnover rates were calculated based on deuterium incorporation into guanosine monophosphate. Data show a large fold changes between 16S and 18s rRNA concentration to not significantly change rRNA turnover rates.

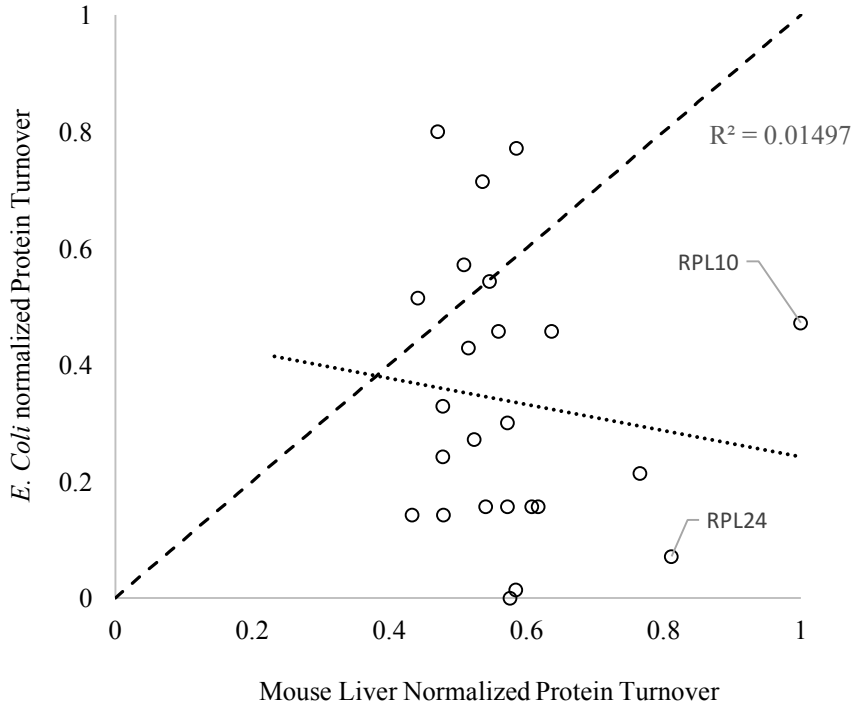

Supplemental Figure 3: *E. coli* ribosomal protein turnover rates do not correlate with mouse liver ribosomal protein turnover rates.

Protein turnover rates were normalized against the fastest turnover ribosomal protein measured within the organism. Simple regression analysis shows no correlation between *E. coli* and *Ad libitum* fed mouse liver turnover.